Microscopic description of low-lying states in deformed nuclei with rotation–vibration coupling

V. O. Nesterenko
Joint Institute for Nuclear Research, Dubna

Fiz. Elem. Chastits At. Yadra **24**, 1517–1550 (November–December 1993)

The extended version of the Quasiparticle–Phonon Model (QPM) for even–even, odd, and odd–odd deformed nuclei is presented. The main new point is allowance for the coupling of rotational and vibrational degrees of freedom. Applications of the model for all three types of nuclei are considered.

1. INTRODUCTION

The present-day status of investigation of low-lying states in deformed nuclei requires the construction of a general microscopic model which would include consistently such important ingredients of the residual interaction as the rotational and vibrational degrees of freedom, the Coriolis mixing, the coupling to even–even core excitations (for odd and odd–odd nuclei), the pairing, and, finally, the interaction between an external proton and neutron in an odd–odd nucleus, which results in the Gallagher–Moszkowski splitting and the Newby shift. It is very important also that the model would be able to describe the properties of even–even, odd, and odd–odd nuclei on the same microscopic footing. Up to now, such a general microscopic model has not been derived, though some ingredients mentioned above have been incorporated into different microscopic models (see, e.g., Refs. 1–8). The QPM (Refs. 1–4, 10, and 11) seems to be the most appropriate ground for this aim, since just the QPM is known to succeed in the description of the vibrational low-lying states in a wide region of deformed even–even and odd nuclei.[1–3,10–17] It is worth noting that in the QPM most of the model parameters are fixed at the stage of calculations for the even–even core. In this sense the calculations in the QPM for even–even, odd, and odd–odd nuclei are consistent.

The investigation of low-lying states in deformed nuclei within the QPM was developed recently in the following directions: two-phonon components in low-lying states of even–even nuclei, the Pauli-principle effects, the particle–particle channel of residual interaction, high-multipolarity states, magnetic collective excitations, and so on. These fields are described in the monograph of Ref. 2 and will not be presented here. The main aim of this paper is a further extension of the QPM by taking into account rotational degrees of freedom together with their coupling (through the Coriolis interaction) to vibrational excitations. It is clear from the very beginning that in deformed nuclei, where rotational and vibrational excitations are in many cases quite entangled, such an extension of the model should be very important for a successful description of low-lying states. Also, additional modifications (mainly for odd–odd nuclei) providing the grounds for the calculation of the Gallagher–Moszkowski splitting, Newby shift, mixing of neutron–proton configurations, and some other effects are proposed. The sketch of a general microscopic scheme for the description of low-lying states in strictly deformed nuclei, which satisfies to a large extent the demands listed above, is given. In the framework of this scheme all degrees of freedom are considered on the same microscopic footing. Such an extended model can be applied to even–even, odd, and odd–odd deformed nuclei. A description of the model is given in Sec. 2.

A practical application of the general scheme presented here is not a simple task. Rather sophisticated computer codes should be used. Now only for odd nuclei the main ingredients of the model (the quasiparticle–phonon and Coriolis interactions) are taken into account simultaneously in real calculations.[18–20] Thus, only for such nuclei is the general scheme realized to a large extent. In calculations for even–even and especially for odd–odd nuclei, truncated versions of the general scheme, embracing only one of the main ingredients, have been used up to now.[1,2,4,13] Nevertheless, we present here examples of calculations for these nuclei also, since in spite of the simplified character of these calculations the results seem to be rather interesting from the physical point of view.

As a first example we will consider in Sec. 3.1 the nonadiabatic behavior of $E2(\gamma \to gr)$ transitions in ^{166}Er, discovered recently in the Coulomb-excitation reaction.[21] In the phenomenological two-rotor model[22] this behavior is explained by the coupling between the γ and ground bands through the $K^\pi = 1^+$ state, interpreted as a "scissors" mode.[23] The Coriolis interaction is considered as the main (but not the only) physical origin of this coupling. We will show that in the framework of the RPA the Coriolis coupling between the ground and 1^+ states vanishes completely if the rotational invariance of the Hamiltonian is restored.[24] This effect has not been mentioned before in spite of the intensive investigation of the "scissors" mode for a long time. Thus, the ground and 1^+ states represent a unique example of states with the same parity and $\Delta K = 1$, which are not mixed by the Coriolis interaction in the framework of the familiar RPA. Under some special conditions, e.g., in the case of nuclear triaxiality, the Coriolis mixing appears again. Thus, the physical interpretation of the phenomenological description[22] is not trivial and needs careful analysis.

The second example presented in Sec. 3.2 concerns odd nuclei. It will be shown that even very small (about 1%) octupole admixtures in wave functions of odd nuclei can

 1063-7796/93/060640-17$10.00

strongly influence $E1$ transitions between low-lying states. This is a challenge to numerous calculations of reduced probabilities $B(E1)$ where only pairing and Coriolis mixing were taken into account (the main motivation for neglecting vibrational admixtures in such calculations was just their small magnitude). Also, it is demonstrated that in some expressive cases only the interplay of the quasiparticle–phonon and Coriolis interactions can explain the experimental data.[18,19]

In Sec. 3.3 calculations for low-lying states of ^{166}Ho are presented, where the coupling of external nucleons to core vibrations is taken into account.[8,9] It turns out that low-lying states contain vibrational components whose magnitudes are sufficiently large to influence strongly the reduced probabilities of electric transitions. This means that, as in odd nuclei, the traditional approach for calculations of $B(E\lambda)$ values in odd–odd nuclei, where only pairing and Coriolis coupling are taken into account, should be revised.

2. THE MODEL

2.1. The Hamiltonian

The Hamiltonian of the model is written as a sum of the rotational, intrinsic, and Coriolis interaction terms:

$$H=H_{\rm rot}+H_{\rm intr}+H_{\rm cor}, \tag{1}$$

where

$$H_{\rm rot}=\frac{h^2}{2J}\cdot(I^2-I_3^2), \tag{2}$$

$$H_{\rm cor}=-\frac{h^2}{2J}\cdot(I^+j^-+I^-j^+). \tag{3}$$

In Eqs. (2)–(3), $I^{\pm}$ and $j^{\pm}$ are the shift operators of the total and intrinsic angular momenta, respectively; K is the projection of the angular momentum onto the z axis; J is the moment of inertia.

In accordance with Refs. 1, 2, 4, and 9,

$$H_{\rm intr}=H_{\rm sp}+H_{\rm pair}+H_{\rm mm}, \tag{4}$$

where $H_{\rm sp}$ is a single-particle potential,

$$H_{\rm pair}=-\sum_{\tau}\sum_{q_1q_2}G_\tau a^\dagger_{q_1^+}a^\dagger_{q_1^-}a_{q_2^-}a_{q_2^+}, \tag{5}$$

is a monopole pairing, and

$$H_{\rm res}=-1/2\sum_{\lambda\tilde\mu}\sum_{\tau\tau'}(\kappa_0^{(\lambda\mu)}+\tau\tau'\kappa_1^{(\lambda\mu)})Q^{(\tau)}_{\lambda\tilde\mu}Q^{(\tau')}_{\lambda-\tilde\mu} \tag{6}$$

is an isoscalar and isovector interaction. In this paper the latter is taken in the form of multipole–multipole forces, except for the special case of consideration of the Gallagher–Moszkowski splitting and Newby shift, where spin–spin forces are used. The use of a spin-multipole residual interaction for the description of magnetic-type excitations in deformed nuclei is considered in Ref. 2 and is not presented here. The multipole operator in (6) is written as

$$Q^{(\tau)}_{\lambda\mu}=\sum_{\tilde q_1\tilde q_2\in\tau}\delta_{\tilde K_1-\tilde K_2,\tilde\mu}\langle\tilde q_1|\hat f^{\lambda\mu}|\tilde q_2\rangle a^\dagger_{\tilde q_1}a_{\tilde q_2}, \tag{7}$$

where $\langle\tilde q_1|\hat f^{\lambda\mu}|\tilde q_2\rangle$ is the single-particle matrix element for the operator

$$\hat f^{\lambda\mu}=R(r)(Y_{\lambda\mu}+(-1)^\mu Y_{\lambda-\mu})(1+\delta_{\mu,0})^{-1} \tag{8}$$

with unspecified radial dependence $R(r)$. In Eqs. (5)–(7), τ is equal to -1 and $+1$ for neutron and proton systems, respectively; $a^\dagger_{\tilde q}$ ($a_{\tilde q}$) is the particle creation (annihilation) operator for the single-particle state $\tilde q$; $\tilde q=q\sigma$, $\tilde K=K\sigma$; $\tilde\mu=\mu\sigma$, $\mu\geqslant0$; $\sigma=\pm1$ characterizes the symmetry with respect to the time-reversal operation; G_τ is the pairing strength constant; $\kappa_0^{(\lambda\mu)}$ and $\kappa_1^{(\lambda\mu)}$ are the strength constants of the isoscalar and isovector interaction, respectively.

Using the RPA equations for one-phonon excitations of the even–even core, the intrinsic Hamiltonian (4) can be transformed to the form

$$H_{\rm intr}=H_{\alpha+Q}+H^{\rm ph}_{QB}+H^{\rm pair}_{QB}+H_{BB}, \tag{9}$$

where

$$H_{\alpha+Q}=\sum_q\varepsilon_qB(qq;0)-1/4\sum_{\lambda\tilde\mu}\sum_\tau\sum_{ii'}\frac{X^g_\tau+X^{g'}_{-\tau}}{\sqrt{\tilde Y^g_\tau\tilde Y^{g'}_\tau}}Q^\dagger_gQ_{\tilde g'} \tag{10}$$

generates quasiparticle and phonon excitations,

$$H^{\rm ph}_{QB}=-1/4\sum_\tau\sum_{\tilde g}\sum_{q_1q_2\in\tau}\Gamma^{\rm ph}_{gq_1q_2}(\tau)\times[(Q^\dagger_g+Q_{-\tilde g})B(q_1q_2;-\tilde\mu)+{\rm h.c.}] \tag{11}$$

is the quasiparticle–phonon interaction in the particle–hole channel (just this interaction couples the quasiparticle excitations of the external nucleons in odd and odd–odd nuclei to the phonon vibrations of the even–even core as well as multiphonon configurations differing from each other by one phonon in even–even nuclei),

$$H^{\rm pair}_{QB}=\sum_\tau\sum_i\sum_{q_1q_2\in\tau}[(\Gamma^{{\rm pair}(+)}_{iq_1q_2}(\tau)Q^\dagger_{20i}+\Gamma^{{\rm pair}(-)}_{iq_1q_2}(\tau)Q_{20i})B(q_1q_2;0)+{\rm h.c.}] \tag{12}$$

is the pairing quasiparticle–phonon interaction, and

$$H_{BB}=-1/2\sum_{\lambda\tilde\mu}\sum_{\tau\tau'}(k_0^{(\lambda\mu)}+\tau\tau'\kappa_1^{(\lambda\mu)})\times\sum_{q_1q_2q_1'q_2'\in\tau}\Gamma^{BB}_{\lambda\mu q_1q_2q_1'q_2'}(\tau)B(q_1q_2;\tilde\mu)B(q_1'q_2';-\tilde\mu) \tag{13}$$

is the so-called "scattering" interaction. In the case of spin–spin residual forces it is just this interaction that is responsible for the Gallagher–Moszkowski splitting and the Newby shift.[8,9]

In (10)–(13) the following notation is used: ε_q is the energy of the one-quasiparticle state q;

$$Q_{\tilde{g}}^{\dagger}=1/2\sum_{q_1q_2}[\psi^{g}_{q_1q_2}A^{\dagger}(q_1q_2;\tilde{\mu})-\phi^{g}_{q_1q_2}A(q_1q_2;-\tilde{\mu})] \tag{14}$$

is the creation operator of the one-phonon state $\tilde{g}\equiv g\sigma\equiv\lambda\mu i\sigma$, where i is the number of one-phonon states with given $\lambda\mu$; $\psi^{g}_{q_1q_2}$ and $\phi^{g}_{q_1q_2}$ are the forward and backward amplitudes of the two-quasiparticle component q_1q_2; the two-quasiparticle operators $A^{\dagger}(q_1q_2;\tilde{\mu})$ and $B(q_1q_2;\tilde{\mu})$ are of the form

$$A^{\dagger}(q_1q_2;\tilde{\mu})=-\frac{1}{\sqrt{1+\delta_{\mu,0}}}\sum_{\sigma_1,\sigma_2}\delta_{\tilde{K}_1+\tilde{K}_2,\tilde{\mu}}\alpha^{\dagger}_{\tilde{q}_1}\alpha^{\dagger}_{\tilde{q}_2}\theta_{\sigma_1-\sigma_2} \tag{15}$$

and

$$B(q_1q_2;\tilde{\mu})=\sum_{\sigma_1,\sigma_2}\delta_{\tilde{K}_1+\tilde{K}_2,\tilde{\mu}}\alpha^{\dagger}_{\tilde{q}_1}\alpha_{-\tilde{q}_2}\theta_{-\sigma_1-\sigma_2}, \tag{16}$$

where $\theta_{-\sigma_1-\sigma_2}=1-\delta_{\sigma_1,1}\delta_{\sigma_2,1}$. The expressions for the functions $\psi^{g}_{q_1q_2}$, $\psi^{g}_{q_1q_2}$, X^{g}_{τ}, Y^{g}_{τ}, $\Gamma^{\rm ph}_{gq_1g_2}(\tau)$, $\Gamma^{\rm pair(+)}_{iq_1q_2}(\tau)$, $\Gamma^{\rm pair(-)}_{iq_1q_2}(\tau)$, and $\Gamma^{BB}_{\lambda\mu q_1q_2q_1'q_2'}(\tau)$ which are determined after solving the RPA equations are given in the Appendix.

2.2. Wave functions for even–even, odd, and odd–odd nuclei

The wave function of the Hamiltonian (1) has the form

$$|I^{\pi}M\rho\rangle=\sum_{K\nu}b^{i\rho}_{\nu K}|I^{\pi}MK\nu\rangle, \tag{17}$$

where $b^{I\rho}_{\nu K}$ are the Coriolis mixing coefficients; M and K are the angular-momentum projections in the laboratory and intrinsic systems, respectively; ρ and ν are additional quantum numbers. Further,[25]

$$|I^{\pi}MK\nu\rangle=\sqrt{\frac{2I+1}{16\pi^2(1+\delta_{K,0})}}\cdot(D^{I}_{MK}+(-1)^{I+K}D^{I}_{M-K}R_i)\cdot\Psi_{\nu}(K^{\pi}), \tag{18}$$

where $\Psi_{\nu}(K^{\pi})$ is the eigenvector of $H_{\rm intr}$; R_i is the operator of rotation by an angle π around the second intrinsic axis.

In this paper the intrinsic wave function for an even–even nucleus is written as a one-phonon state

$$\Psi_{\tilde{g}}(\tilde{K}^{\pi})=Q^{\dagger}_{\tilde{g}}|\rangle_{\rm RPA}, \tag{19}$$

though the two-phonon version[2,26] (or the multiphonon one[27]) of the wave function may also be used. The case when the wave function of an even–even nucleus contains both one- and two-phonon components is described in detail in Ref. 2 and is not considered here.

In an odd nucleus the intrinsic wave function has the form[1,2,4]

$$\Psi_{\nu}(\tilde{K}^{\pi})=\left\{\sum_{\tilde{q}_1}C^{\nu}_{q_1}\delta_{\tilde{K}_1,\tilde{K}}\alpha^{\dagger}_{\tilde{q}_1}+\sum_{\tilde{q}_1\tilde{g}_1}D^{\nu}_{q_1g_1}\delta_{\tilde{K}_1+\tilde{\mu}_1,\tilde{K}}\alpha^{\dagger}_{\tilde{q}_1}Q^{\dagger}_{\tilde{g}_1}\right\}|\rangle_{\rm RPA}|\rangle_q, \tag{20}$$

where $C^{\nu}_{q_1}$ and $D^{\nu}_{q_1g_1}$ are the amplitudes of the one-quasiparticle and quasiparticle ⊗ phonon components, respectively; $|\rangle_{\rm RPA}$ and $|\rangle_q$ are the RPA ($Q_{\tilde{g}}|\rangle_{\rm RPA}=0$) and quasiparticle ($\alpha_{\tilde{q}}|\rangle_q=0$) vacuum; ν is the number of the state with given K^{π}.

In an odd–odd nucleus the intrinsic wave function is[4,8,9]

$$\Psi_{\nu\gamma}(\tilde{K}^{\pi})=\left\{\sum_{\tilde{s}_1\tilde{r}_1}C^{\nu\gamma}_{s_1r_1}A^{\dagger}_{\gamma}(\tilde{s}_1\tilde{r}_1\tilde{K})+\sum_{\tilde{s}_1\tilde{r}_1\tilde{g}_1\gamma_1}\times k^{K}_{\mu}D^{\nu\gamma_1}_{s_1r_1g_1}A^{\dagger}_{\gamma_1}(\tilde{s}_1\tilde{r}_1\tilde{K}_1)Q^{\dagger}_{\tilde{g}_1}\delta_{\tilde{K}_1+\tilde{\mu},\tilde{K}}\right\}|\rangle_{\rm RPA}|\rangle_q, \tag{21}$$

where

$$A^{\dagger}_{\gamma}(\tilde{s}\tilde{r}\tilde{K})=\frac{1}{\sqrt{1+\delta_{K,0}}}\alpha^{\dagger}_{\tilde{s}}\alpha^{\dagger}_{\tilde{r}}\delta_{\tilde{K}_s+\tilde{K}_r,\tilde{K}}k^{K}_{\gamma\sigma_s\sigma_r} \tag{22}$$

and

$$k^{K}_{\mu}=[1+\delta_{K,0}(1-\delta_{\mu,0})]^{-1/2},$$
$$k^{K}_{\gamma\sigma_s\sigma_r}=1-(1+\gamma)\delta_{K,0}\delta_{\sigma_s,-1}\delta_{\sigma_r,+1}. \tag{23}$$

Here, $C^{\nu\gamma}_{s_1r_1}$ and $D^{\nu\gamma}_{s_1r_1g_1}$ are the amplitudes of the neutron–proton and neutron–proton ⊗ phonon components, respectively. For $K=0$ the function (21) depends on $\gamma=\pm1$, which is the eigenvalue of the operator R_i. In this case the condition $\gamma=(-1)^I$ holds.[25] The coefficients k^K_{μ} and $k^{K}_{\gamma\sigma_s\sigma_r}$ are introduced to provide a simple form of the normalization condition for the wave function (21).[8,9]

After solving the RPA equations for the even–even core the phonon basis is used for the construction of the states (20)–(21). The energies and structure of the intrinsic states (20)–(21) are calculated by the variational method with retention of the normalization condition for the states. It should be noted that all the parameters of the model are fixed after solving the RPA equations.

If a wave function includes complex components like two-phonon (in even–even nuclei, quasiparticle ⊗ phonon; in odd nuclei, neutron–proton ⊗ phonon), in odd–odd nuclei we should take into account the Pauli principle. This problem was considered for even–even and odd nuclei in Refs. 2, 3, 10, and 27. In Ref. 27 it was shown for even–even nuclei that allowance for multiphonon configurations (three-phonon, and so on) decreases to a large extent the excitation energy shifts caused by the Pauli-principle effects. For the sake of brevity we do not present here the corresponding formalism.

2.3. Final expressions of the model

The RPA equations for one-phonon excitation in even–even nuclei are given in the Appendix. Below, we present the final expressions for determining the wave functions and excitation energies in odd and odd–odd nuclei. These expressions are derived in the framework of the variational procedure.[1-3,8,9] Since we do not discuss in this paper the Pauli-principle effects, the corresponding corrections are omitted.

For odd nuclei the amplitudes C_q^ν and D_{qg}^ν of the wave function (20) are found from the system of equations

$$\sum_{q'} C_{q'}^\nu \left\{ (\varepsilon_q-\eta_\nu)\delta_{q,q'} - \frac{1}{4}\sum_{gq_1} \frac{\Gamma_{gq_1q}(\tau)\Gamma_{gq_1q'}(\tau)}{\varepsilon_{q_1}+\omega_g-\eta_\nu} \right\}=0, \tag{24}$$

$$D_{qg}^\nu=(\varepsilon_q+\omega_g-\eta_\nu))^{-1}\cdot\frac{1}{2}\sum_{q'} C_{q'}^\nu \Gamma_{gqq'}(\tau), \tag{25}$$

and the secular equation for determination of the excitation energy η_ν is

$$\det\left\| (\varepsilon_q-\eta_\nu)\delta_{q,q'} - \frac{1}{4}\sum_{gq_1} \frac{\Gamma_{gq_1q}(\tau)\Gamma_{gq_1q'}(\tau)}{\varepsilon_{q_1}+\omega_g-\eta_\nu} \right\|=0. \tag{26}$$

For odd–odd nuclei the corresponding equations are

$$\sum_{s'r'} C_{s'r'}^{\nu\gamma} \left\{ (\varepsilon_s+\varepsilon_r+\langle rs|V_{np}|rs\rangle_{0\gamma}-\eta_\nu)\delta_{sr,s'r'} - \frac{1}{4}\sum_{gs_1r_1\gamma'} \times\frac{\Gamma_{gss_1rr_1}\Gamma_{gs's_1r'r_1}}{\varepsilon_{s_1}+\varepsilon_{r_1}+\langle r_1s_1|V_{np}|r_1s_1\rangle_{\mu\gamma}+\omega_g-\eta_{\nu\gamma}} \right\}=0, \tag{27}$$

$$D_{srg}^{\nu\gamma}=(\varepsilon_s+\varepsilon_r+\langle rs|V_{np}|rs\rangle_{\mu\gamma}+\omega_g-\eta_{\nu\gamma})^{-1} \times\frac{1}{2}\sum_{s'r'} C_{s'r'}^{\nu\gamma}\Gamma_{gss'rr'} \tag{28}$$

and

$$\det\left\| (\varepsilon_s+\varepsilon_r+\langle rs|V_{np}|rs\rangle_{0\gamma}-\eta_\nu)\delta_{sr,s'r'} - \frac{1}{4}\sum_{gs_1r_1\gamma'} \frac{\Gamma_{gss_1rr_1}\Gamma_{gs's_1r'r_1}}{\varepsilon_{s_1}+\varepsilon_{r_1}+\langle r_1s_1|V_{np}|r_1s_1\rangle_{\mu\gamma}+\omega_g-\eta_{\nu\gamma}} \right\|=0, \tag{29}$$

where

$$\Gamma_{gss_1rr_1}=\Gamma_{gss_1}(\tau=-1)\delta_{r,r_1}+\Gamma_{grr_1}(\tau=+1)\delta_{s,s_1}. \tag{30}$$

In (27)–(29) only diagonal matrix elements of the n–p interaction $\langle rs|V_{np}|rs\rangle_{\mu\gamma}$ are taken into account. These matrix elements are discussed in Sec. 2.5. Except for the n–p interaction terms the final equations for odd and odd–odd nuclei are quite similar. The expression for $\Gamma_{gqq_1}(\tau)$ is given in the Appendix.

2.4. *Eλ* transition probabilities

The reduced probability of an $E\lambda$ transition between the states (17) is written as[25]

$$B(E\lambda,I_\rho^\pi\to I_{\rho'}^{\pi'})=1/(2I+1)\,|\langle I_{\rho'}^{\pi'}\|E\lambda\|I_\rho^\pi\rangle|^2, \tag{31}$$

where the reduced matrix element has the form

$$\langle I_{\rho'}^{\pi'}\|E\lambda\|I_\rho^\pi\rangle=\sqrt{2I+1}\sum_{K\nu K'\nu'} b_{\nu K}^{I\rho}b_{\nu'K'}^{I'\rho'}\{(IK\lambda K'-K|I'K')(\Psi_{\nu'}(K'^{\pi'})\hat{M}(E\lambda,\mu=K'-K)\Psi_\nu(K^\pi))+(-1)^{I+K}(I-K\lambda K'+K|I'K')(\Psi_{\nu'}(K'^{\pi'})\hat{M}(E\lambda,\mu=K'+K)\Psi_\nu(K^\pi))\}. \tag{32}$$

The intrinsic matrix element $(\Psi_{\nu'}(K'^{\pi'})\hat{M}(E\lambda,\mu=K'\pm K)\Psi_\nu(K^\pi))$ is calculated using the operator for the $E\lambda$ transition:[2,10]

$$\hat{M}(E\lambda,\tilde{\mu})=\sum_i L_g^{E\lambda}(Q_{\tilde{g}}^\dagger+Q_{-\tilde{g}}) + \sum_{q_1q_2} p_{q_1q_2}^{\lambda\mu}v_{q_1q_2}^{(-)}B(q_1q_2;\tilde{\mu})+2\sum_q p_{qq}^{\lambda\mu}v_q^2. \tag{33}$$

Here

$$L_g^{E\lambda}=\sqrt{(1+\delta_{\mu,0})/4}\sum_{q_1q_2} p_{q_1q_2}^{\lambda\mu}u_{q_1q_2}^{(+)}(\psi_{q_1q_2}^g+\phi_{q_1q_2}^g) \tag{34}$$

is the matrix element of the $E\lambda$ transition between the one-phonon state (19) and the ground state; $v_{q_1q_2}^{(\pm)}=u_{q_1}u_{q_2}\pm v_{q_1}v_{q_2}$ and $u_{q_1q_2}^{(\pm)}=u_{q_1}v_{q_2}\pm v_{q_1}u_{q_2}$; u_q and v_q are the Bogolyubov transformation coefficients; $p_{q_1q_2}^{\lambda\mu}$ is the single-particle matrix element for the operator of the $E\lambda$ transition:

$$\hat{p}=ee_{\text{eff}}^\tau r^\lambda(Y_{\lambda\mu}+(-1)^\mu Y_{\lambda-\mu})(1+\delta_{\mu,0})^{-1}, \tag{35}$$

where the effective charge $e_{\text{eff}}^\tau=(1+\tau)/2+e_{\text{eff}}$ is fitted so as to reproduce the experimental $B(E\lambda)$ values in the even–even core.

The first term in Eq. (33) is responsible for the $E\lambda$ transitions between the states (or components of the states) which differ from each other by one phonon. This term determines the transitions between the ground and one-phonon states in the even–even core and the collective part of the interband $E\lambda$ transitions in odd and odd–odd nuclei. The second term in (33) determines $E\lambda$ transitions between the wave-function components with the same number of quasiparticles (phonons). This term plays the main role in interband transitions in odd and odd–odd nuclei if vibrational admixtures of wave functions can be neglected. The third term in (33) is responsible for the intraband transitions. It is this term that determines the quadrupole moment of the nucleus.

The intrinsic matrix elements for odd and odd–odd nuclei are, respectively,

$$[\Psi_{\nu'}(K'^{\pi'})\hat{M}(E\lambda,\mu=K'\pm K)\Psi_\nu(K^\pi)] = \sum_{qq'} C_q^\nu C_{q'}^{\nu'} v_{qq'}^{(-)}\tilde{p}_{qq'}^{\lambda\mu}$$

$$+\sum_i L^{E\lambda}_{\lambda\mu i}\sum_{q_1}(C^{\nu'}_{q'}D^{\nu}_{q_1g}+D^{\nu'}_{q_1g}C^{\nu}_{q})$$

$$+\sum_{g_1}\sum_{q_1g_1'}D^{\nu}_{q_1g_1}D^{\nu'}_{q_1'g_1}v^{(-)}_{q_1q_1'}\tilde{p}^{\lambda\mu}_{q_1q_1'} \quad (36)$$

and

$$[\Psi_{\nu'\gamma'}(K'^{\pi'})\hat{M}(E\lambda,\mu=K'\pm K)\Psi_{\nu\gamma}(K^{\pi})]$$

$$=\sum_{ss'rr'}C^{\nu\gamma}_{sr}C^{\nu\gamma'}_{s'r'}(v^{(-)}_{ss'}\tilde{p}^{\lambda\mu}_{ss'}\delta_{r,r'}+v^{(-)}_{rr'}\tilde{p}^{\lambda\mu}_{rr'}\delta_{s,s'})k^{CC}_{\gamma\gamma'}$$

$$+\sum_i L^{E\lambda}_{\lambda\mu i}\sum_{sr}(C^{\nu'\gamma'}_{sr}D^{\nu\gamma}_{srg}+D^{\nu'\gamma'}_{srg}C^{\nu\gamma}_{sr})$$

$$+\sum_{ss'rr'}\sum_{g_1}\sum_{\gamma_1\gamma_1'}D^{\nu'\gamma_1}_{srg_1}D^{\nu'\gamma_1'}_{s'r'g_1}(v^{(-)}_{ss'}\tilde{p}^{\lambda\mu}_{ss'}\delta_{r,r'}$$

$$+v^{(-)}_{rr'}\tilde{p}^{\lambda\mu}_{rr'}\delta_{s,s'})k^{DD}_{\gamma_1\gamma_1'}. \quad (37)$$

Expressions for the coefficients $k^{CC}_{\gamma\gamma'}$ and $k^{DD}_{\gamma\gamma'}$ are given in the Appendix. The single-particle matrix element $\tilde{p}^{\lambda\mu}_{qq'}$ of the operator (35) has the same form as the matrix element $\tilde{f}^{\lambda\mu}_{qq'}$, whose expression is also given in the Appendix.

2.5. Gallagher–Moszkowski splitting (GMS) and Newby shift (NS)

It is well known that the GMS and NS in an odd–odd nucleus are caused by the spin–spin part of the interaction between the external neutron and proton. Let us consider the neutron–proton part of the interaction (13) for the case of spin–spin residual forces. It is easy to show that the GMS and NS are implicity involved in the equations for the intrinsic excitations of odd–odd nuclei precisely because of this term.[8,9] Thus, for odd–odd nuclei this term (denoted by V_{np}) should be taken into account in addition to the quasiparticle–phonon interaction.

The expressions for the Gallagher–Moszkowski splitting and Newby shift can be extracted from the secular equation (29) if the long-range residual interaction, except for V_{np}, is neglected $[\Gamma^{\rm ph}_{gq_1q_2}(\tau) = \Gamma^{{\rm pair}(-)}_{iq_1q_2}(\tau) = 0]$. Then for the general case of V_{np} to be Hermitian and invariant under time reversal the secular equation (29) can be written as[8,9]

$$\eta_{\nu\gamma}=\varepsilon_s+\varepsilon_r+\langle rs|V_{np}|rs\rangle_{0\gamma}$$

$$=\varepsilon_s+\varepsilon_r-\delta_{K,0}\gamma\langle r+s-|V_{np}|r-s+\rangle+\delta_{K_s+K_r,K}$$

$$\times[\langle r+s+|V_{np}|r+s+\rangle(u_r^2u_s^2+v_r^2v_s^2)-\langle r-s$$

$$+|V_{np}|r-s+\rangle(v_r^2u_s^2+u_r^2v_s^2)]+\delta_{|K_s-K_r|,K}$$

$$\times[\langle r+s-|V_{np}|r+s-\rangle(u_r^2u_s^2+v_r^2v_s^2)-\langle r-s$$

$$-|V_{np}|r-s-\rangle(v_r^2u_s^2+u_r^2v_s^2)]. \quad (38)$$

Using the connection $\gamma=(-1)^I$, we finally obtain the well-known expression for the Gallagher–Moszkowski splitting energy, corresponding to the case of independent quasiparticles:

$$\Delta E=\eta_{\nu\gamma}\delta_{|K_s-K_r|,K}-\eta_{\nu\gamma}\delta_{K_s+K_r,K}$$

$$=\langle r+s-|V_{np}|r+s-\rangle-\langle r+s+|V_{np}|r+s+\rangle$$

$$+\delta_{K,0}(-1)^{I+1}\langle r+s-|V_{np}|r-s+\rangle. \quad (39)$$

The last term in (39) is connected with the Newby shift:

$$\Delta E_{K=0}=\eta_{\nu\gamma=-1}-\eta_{\nu\gamma=+1}=2\langle r+s-|V_{np}|r-s+\rangle. \quad (40)$$

The expressions (38)–(40) were derived for a general case of V_{np}. The same kind of spin splitting should also occur in even–even nuclei. If the neutron–proton interaction is approximated by (13) with spin–spin forces, the expressions for the energy splitting between two-quasiparticle configurations with parallel and antiparallel spins has an especially simple form:

$$\Delta E=-\tilde{\kappa}^{10}_1\sigma_1\sigma_2\omega^{10}_{q_1q_1}\omega^{10}_{q_2q_2} \quad (41)$$

for the two-quasiparticle state q_1q_2 in an even–even nucleus, and

$$\Delta E=+\tilde{\kappa}^{10}_1\sigma_s\sigma_r\omega^{10}_{ss}\omega^{10}_{rr} \quad (42)$$

for the neutron–proton state sr in an odd–odd nucleus. In (41)–(42), $\tilde{\kappa}^{10}_1$ is the strength constant of the isovector spin–spin interaction with multipolarity $\lambda\mu=10$ (this strength constant is negative); ω^{10}_{ss} is a diagonal single-particle matrix element for the Pauli matrix operator; the σ values are defined here as the signs of the K projections (do not confuse them with the signs of the spin projections!). The calculations for rare-earth even–even nuclei[28] have shown that the expression (41) reproduces well the Gallagher rule for even–even nuclei. This rule states that the two-quasiparticle configuration has a lower excitation energy if the spins of the quasiparticles are antiparallel than in the case of parallel spins.

2.6. Coriolis-interaction matrix elements

The general expression (for even–even, odd, and odd–odd nuclei) for the Coriolis matrix element is

$$\langle|I'^{\pi}M'K'\nu'|H_{\rm cor}|I^{\pi}MK\nu\rangle=$$

$$-\delta_{I'M',IM}\frac{h^2}{2J}\Big\{\delta_{K',K-1}\sqrt{1+\delta_{K',0}}\sqrt{(I+K)(I-K+1)}$$

$$\times(\Psi_{\nu'}(K'^{\pi})|j^-|\Psi_{\nu}(K^{\pi}))$$

$$+\delta_{K',K+1}\sqrt{1+\delta_{K',0}}\sqrt{(I-K)(I+K+1)}$$

$$\times(\Psi_{\nu'}(K'^{\pi})|j^+|\Psi_{\nu}(K^{\pi}))+(-1)^{I+1/2}$$

$$\times\delta_{K,1/2}\delta_{K',1/2}\Big(\Psi_{\nu'}\Big(K'^{\pi}=\frac{1^+}{2}\Big)\Big|j^+\Big|\Psi_{\nu}\Big(K^{\pi}=\frac{1^-}{2}\Big)\Big)\Big\}. \quad (43)$$

In the simplest case of one-phonon excitations (19) in even–even nuclei the intrinsic matrix element $(\Psi_{\nu'}(K'^{\pi})|j^+|\Psi_\nu(K^\pi))$ is written as

$$\langle K'^{\pi}_{\nu'}=1^+_\nu|j^+|\rangle_{\rm RPA}\equiv{}_{\rm RPA}\langle|Q_{21\nu}j^+|\rangle_{\rm RPA}$$

$$=\sum_{q_1>q_2} j^+_{q_1q_2}u^{(-)}_{q_1q_2}(\psi^{21\nu}_{q_1q_2}+\phi^{21\nu}_{q_1q_2}) \tag{44}$$

for the coupling between the ground and 1^+_ν bands and

$$\langle K'^{\pi}_{\nu'}|j^+|K^\pi_\nu\rangle\equiv{}_{\rm RPA}\langle|Q_{\lambda'\mu'\nu'}j^+Q^\dagger_{\lambda\mu\nu}|\rangle_{\rm RPA}$$

$$=\delta_{K',K+1}\sum_{q_1>q_2} j^+_{q_1q_2}v^{(+)}_{q_1q_2}\sum_{q_3}(\psi^{\lambda'\mu'\nu'}_{q_1q_3}\psi^{\lambda\mu\nu}_{q_2q_3}+\psi^{\lambda'\mu'\nu'}_{q_3q_2}\psi^{\lambda\mu\nu}_{q_3q_1})(1+\delta_{K_1+K_2,1}) \tag{45}$$

for the coupling between bands with one-phonon band heads (the γ and 1^+_ν bands, octupole bands, and so on). In (44) and (45) the boson ($\sim a^\dagger_{q_1\sigma_1}a^\dagger_{q_2\sigma_2}$) and fermion ($\sim a^\dagger_{q_1\sigma_1}a_{q_2\sigma_2}$) parts of the operator j^+ are taken into account, respectively; $j^+_{q_1q_2}$ is the single-particle matrix element for this operator.

It is easy to see that the well-known condition of restoration of the rotational invariance in even–even nuclei

$$\langle 1^+_\nu|I^+|\rangle_{\rm RPA}\equiv{}_{\rm RPA}\langle|Q_{21\nu}I^+|\rangle_{\rm RPA}=0 \tag{46}$$

in the intrinsic system can be written as

$$\langle 1^+_\nu|j^+|\rangle_{\rm RPA}\equiv{}_{\rm RPA}\langle|Q_{21\nu}j^+|\rangle_{\rm RPA}=0, \tag{47}$$

since in this case only the intrinsic part of the total momentum operator affects the RPA wave functions. As a result, Eq. (47) for the Coriolis matrix element has the same form as the relation of the orthogonality of the RPA wave function to the spurious state in Ref. 29. Equation (47) leads to an important consequence: if in the RPA calculations the rotational invariance is restored correctly, the Coriolis interaction between the ground band and the $K^\pi=1^+_\nu$ bands should be exactly zero. For the case of two-quasiparticle states (without a residual interaction) a similar result has been obtained in Ref. 30. Thus, in the framework of the RPA the ground band has no Coriolis coupling to any other band. It should be noted that under some special conditions (for example, triaxiality of the nucleus) the Coriolis coupling of the ground band to the $K^\pi=1^+_\nu$ bands appears again.

The intrinsic matrix elements of the Coriolis interaction for odd and odd–odd nuclei are, respectively,

$$(\Psi_{\nu'}(K'^{\pi})|j^+|\Psi_\nu(K^\pi))$$

$$=\sum_{qq'}C^\nu_qC^{\nu'}_{q'}v^{(+)}_{qq'}\tilde{j}^+_{qq'}+\sum_{g_1}\sum_{q_1q'_1}D^\nu_{q_1g_1}D^{\nu'}_{q_1g_1}v^{(+)}_{q_1q'_1}\tilde{j}^+_{q_1q'_1} \tag{48}$$

and

$$[\Psi_\nu(K^\pi)|j^+|\Psi_{\nu'}(K'^{\pi})]$$

$$=\sum_{ss'rr'}C^{\nu\gamma}_{sr}C^{\nu\gamma'}_{s'r'}(v^{(+)}_{rr'}\tilde{j}^+_{ss'}\delta_{r,r'}+v^{(+)}_{rr'}\tilde{j}^+_{rr'}\delta_{s,s'})k^{CC}_{\gamma\gamma'}$$

$$+\sum_{ss'rr'}\sum_{g_1}\sum_{\gamma_1\gamma'_1}D^{\nu'\gamma_1}_{srg_1}D^{\nu'\gamma'_1}_{s'r'g_1}(v^{(+)}_{ss'}\tilde{j}^+_{ss'}\delta_{r,r'}+v^{(+)}_{rr'}\tilde{j}^+_{rr'}\delta_{s,s'})k^{DD}_{\gamma_1\gamma'_1}. \tag{49}$$

Note that terms of the type $C^\nu\cdot D^{\nu'}$ are absent in (48) and (49). This is the case if we take into account the rotational invariance of the Hamiltonian (see the above comment for even–even nuclei) and neglect the Pauli-principle effects.

In Ref. 31 it has been shown that vibrational admixtures in wave functions of odd deformed nuclei can be the main reason for the well-known attenuation of the Coriolis-coupling matrix elements. Indeed, vibrational admixtures in the wave function of an odd nucleus (20) decrease the absolute values of the amplitudes C^ν_q of one-quasiparticle configurations. As a result, if the heads of two rotational bands can be approximated by one-quasiparticle configurations q_1 and q_2, we can easily get in a first approximation the following attenuation coefficient (caused by vibrational admixtures only!) for the Coriolis coupling between these bands:

$$k^{\rm att}_{q_1q_2}=C^{\nu_1}_{q_1}\cdot C^{\nu_2}_{q_2}. \tag{50}$$

In Sec. 4 this coefficient will be used to estimate the Coriolis attenuation in odd Eu and Tb isotopes. It is clear that a similar attenuation coefficient should also occur for odd–odd nuclei.

3. NONADIABATIC BEHAVIOR OF $E2(\gamma\to gr)$ TRANSITIONS IN ^{166}Er

An almost complete set of reduced $E2$ matrix elements for the ground and γ bands up to spin 14^+ and 12^+, respectively, has recently been measured for ^{166}Er in a Coulomb-excitation experiment.[21] In total, 44 $E2$ matrix elements have been determined in a model-independent way. Some of them clearly show a nonadiabatic behavior (deviation from the Alaga rule). Calculations of the $E2$ matrix elements were performed[21] within four collective models: the symmetrical rotor model, the asymmetric rotor model,[32] the rotation–vibration model,[33] and the IBA-1 model.[34] It has been shown that both the γ deformation and rotation–vibration coupling may be responsible for the strong slope in the $I_\gamma\to(I-2)_{gr}$ transitions (see Fig. 1, taken from Ref. 21). However, these models failed to explain the sudden increase of the $E2$ matrix element of the $10^+_\gamma\to8^+_{gr}$ transition.

The Dubna group has previously succeeded in describing the nonadiabatic effects of the $E2$ transitions between the γ and ground bands [hereafter denoted by $E2(\gamma\to gr)$] in the framework of the two-rotor[22] and Coriolis-coupling[35] phenomenological models. In both models the coupling between the γ and ground bands occurs as a result of the 1^+ state, interpreted as a "scissors" mode.[23] In the latter model the Coriolis interaction is considered as the origin of this coupling. Both models use the

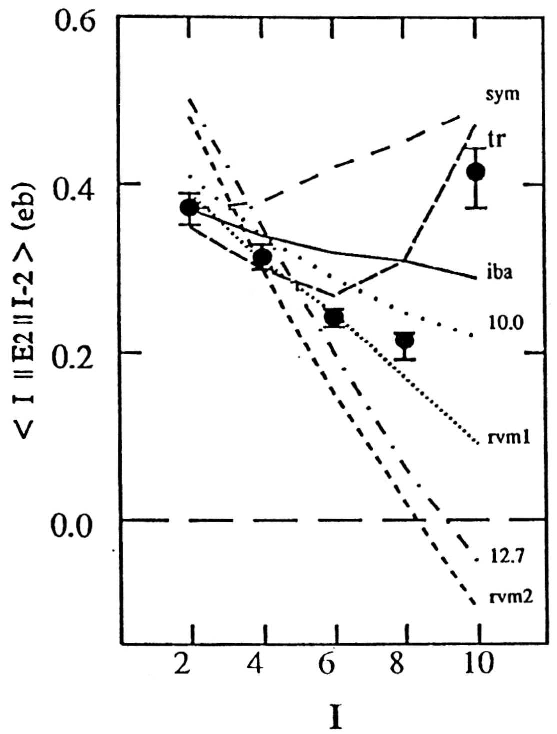

FIG. 1. The experimental and calculated values[21] of the $I_\gamma \to (I-2)_{gr}$ matrix elements in ^{166}Er. The calculations were performed in the symmetric rotor model (sym), the asymmetric rotor model[32] ($\gamma=10°$ and 12.7°, respectively), the rotation–vibration model[33] (rvm1 and rvm2), the IBA-1 model[34] (iba), and a two-rotor model[22] (tr). The adiabatic behavior corresponds to the results of the symmetric rotor model.

band head energies, moments of inertia, the band-coupling matrix elements, and some basic $E2$ matrix elements as parameters fitted so as to reproduce the experimental data for the spectrum and electromagnetic transitions. In some sense the models take into account, through these parameters, the γ deformation. Figure 1 shows that the calculations[22] give a satisfactory description of the experimental data for ^{166}Er.

The main idea of the model,[35] i.e., the Coriolis coupling between the γ and ground bands through one 1^+ state, seems to be attractive. However, the energy excitation interval 2–5 MeV embracing the "scissors" mode includes a large number of 1^+ states. Thus, it is worth performing a microscopic study of the role of the Coriolis coupling in the nonadiabatic behavior of the $E2(\gamma \to gr)$ transitions, taking into account all the 1^+ states in this energy interval and not using any free parameters. The γ deformation is not taken into account, since this would result in rather cumbersome calculations. It is worth noting that although the "scissors" mode has been investigated very carefully (see the review of Ref. 36 and references therein), the problem discussed here has not been considered on a microscopic footing.

The RPA calculations have been performed within the model described in the previous section. The intrinsic Hamiltonian (4) includes the Woods–Saxon single-particle potential as a sum of the spherical and quadrupole parts

$$H_{sp}=V_{WS}^{(0)}(r)+V_{WS}^{(2)}(r)\,Y_{20}(\theta,\varphi), \tag{51}$$

the monopole pairing, and the quadrupole isoscalar and isovector interaction with $\lambda\mu=22$ and 21.[2,10]

The reduced matrix element (32) for the $E2$ transition between the γ and ground bands can be written as

$$\langle I_{gr}^+\|E2\|I_\gamma^+\rangle=\sqrt{2I_\gamma+1}\,(M(E2)_{Q_0}+M(E2)_{1^+}+M(E2)_\gamma), \tag{52}$$

where

$$M(E2)_{Q_0}=\sqrt{\frac{5}{16\pi}}\,eQ_0\left\{\sum_{\rho=gr,\gamma} b_\rho^{I_{gr}} b_\rho^{I_\gamma} C_{I_\gamma K_\rho;20}^{I_{gr}K_\rho} + \sum_{\nu=1} b_{1_\nu^+}^{I_{gr}} b_{1_\nu^+}^{I_\gamma} C_{I_\gamma 1;20}^{I_{gr}1}\right\}, \tag{53}$$

$$M(E2)_{1^+}=\sqrt{2}\sum_{\nu=1} L_{1_\nu^+}^{E2}\{b_{gr}^{I_{gr}} b_{1_\nu^+}^{I_\gamma} C_{I_\gamma 1;2-1}^{I_{gr}0} - b_{1_\nu^+}^{I_{gr}} b_{gr}^{I_\gamma} C_{I_\gamma 0;21}^{I_{gr}1}\}, \tag{54}$$

$$M(E2)_\gamma=\sqrt{2}L_\gamma^{E2}\{b_{gr}^{I_{gr}} b_\gamma^{I_\gamma} C_{I_\gamma 2;2-2}^{I_{gr}0} + b_\gamma^{I_{gr}} b_{gr}^{I_\gamma} C_{I_\gamma 0;22}^{I_{gr}2}\}. \tag{55}$$

In Eq. (53), Q_0 is the quadrupole moment calculated in the microscopic way (see Sec. 2.4).

In the calculations the γ-vibrational $K^\pi=2^+$ state and 30 $K^\pi=1^+$ RPA states (all 1^+ states with excitation energies up to 5 MeV) have been taken into account. Without going into the details of the calculations, which can be found in Ref. 24, let us consider the most delicate point of the task—the determination of the isoscalar strength constant $\kappa_0^{(21)}$, which is known to be connected with the problem of extraction of the spurious admixtures caused by the violation of the rotational invariance of the Hamiltonian. There are different prescriptions for the extraction of the spurious admixtures (see, for example, Refs. 29, 30, 37, and 38). We used the method proposed in Ref. 37, which seems to be the most simple and convenient one if the single-particle potential has the form (51). It is easy to show that in this case the restoration of the rotational invariance leads just to the $\lambda\mu=21$ residual interaction with the radial dependence

$$R_{21}(r)=V_{WS}^{(2)}(r). \tag{56}$$

Indeed, for a single-particle potential of the form

$$H_{sp}=-V_0\sum_{\lambda=0,2,4,\ldots} F_\lambda(r)\,Y_{\lambda 0}(\theta,\phi) \tag{57}$$

we have

$$[H_{sp},I_\nu]=-\nu V_0\sum_{\lambda=0,2,4,\ldots\,\nu=\pm1}\sqrt{\frac{\lambda(\lambda+1)}{2}}\,F_\lambda(r)\,Y_{\lambda\nu}(\theta,\phi), \tag{58}$$

and the rotational invariance violated by the single-particle potential (57) can be restored by the quadrupole residual interaction with the radial dependence (56). The isoscalar strength constant should be adjusted so as to put the first solution of the secular equation for the 1^+ states equal to

TABLE I. Coriolis mixing coefficients for the γ band.

I	$b^{I_\gamma}_{1^+_\nu}$								
	1^+_1	1^+_7	1^+_8	1^+_{11}	1^+_{13}	1^+_{17}	1^+_{22}	1^+_{23}	γ
2	−.0277	−.0137	−.0076	−.0116	.0071	−.0066	.0063	−.0127	.9992
3	−.0426	−.0212	−.0118	−.0180	.0109	−.0105	.0097	−.0181	.9981
4	−.0554	−.0276	−.0153	−.0234	.0142	−.0137	.0127	−.0236	.9968
5	−.0667	−.0334	−.0185	−.0283	.0172	−.0165	.0153	−.0285	.9953
6	−.0768	−.0386	−.0214	−.0327	.0199	−.0191	.0177	−.0330	.9938
7	−.0860	−.0433	−.0241	−.0368	.0223	−.0215	.0199	−.0371	.9922
8	−.0942	−.0476	−.0265	−.0405	.0246	−.0236	.0219	−.0408	.9906
9	−.1017	−.0516	−.0287	−.0439	.0266	−.0256	.0238	−.0443	.9889
10	−.1085	−.0552	−.0307	−.0470	.0285	−.0274	.0255	−.0475	.9873
11	−.1147	−.0586	−.0326	−.0499	.0303	−.0292	.0271	−.0504	.9858
12	−.1205	−.0618	−.0344	−.0526	.0319	−.0307	.0286	−.0532	.9842

zero. For the generalization of this method to the case of both isoscalar and isovector interactions we followed the prescription of Ref. 38. In accordance with Ref. 38, the $\lambda\mu=21$ residual interaction is written as

$$H_{QQ}=-1/2\sum_{T=0,1}\kappa_T^{(21)}\tilde{Q}^\dagger_{21}\tilde{Q}_{21}, \qquad (59)$$

where $\tilde{Q}_{21}=Q^n_{21}+Q^p_{21}$ and $Q^n_{21}-\gamma Q^p_{21}$ for $T=0$ and 1, respectively, and

$$\gamma=\frac{\langle|[Q^n_{21},I_x]|\rangle}{\langle|[Q^p_{21},I_x]|\rangle}. \qquad (60)$$

Then the isoscalar and isovector interactions are decoupled, and the strength constant of the isovector interaction can be fitted so as to reproduce the energy of the isovector giant quadrupole resonance. In this case we have $\kappa_1^{(2\mu)}=-1.5\kappa_0^{(2\mu)}$.

The Coriolis matrix elements that we need for the calculations have the form (44)–(45). If in the RPA calculations the rotational invariance is restored correctly, the Coriolis interaction between the ground band and the $K^\pi=1^+_\nu$ bands should be exactly zero. For the case of two-quasiparticle states (without a residual interaction) a similar result has been obtained in Ref. 30. Thus, in the framework of this approach the 1^+_ν bands are coupled by the Coriolis interaction to the γ band only. The ground band is coupled neither to the γ band nor to the 1^+_ν bands. In this case, $M(E2)_{Q_0}=0$, whereas $M(E2)_{1^+}$ and $M(E2)_\gamma$ contain the first terms only, and the influence of the Coriolis coupling should be rather weak, as is confirmed by our calculations presented below. To switch on the coupling of the ground band to the 1^+_ν and γ band, it is necessary to generalize the approach by, e.g., taking into account a γ deformation.[32]

Let us consider the results of the calculations. In Table I the largest Coriolis mixing coefficients for the γ band are given. The mixing with the 1^+_ν states is shown to be noticeable for both the low-lying and high-lying (the "scissors"-mode region) states.

It is interesting to compare the collectivity of the 1^+_ν states from the low-energy and "scissors"-mode regions. For this purpose the $B(E2,0^+0_{gr}\rightarrow 2^+K_\nu)$ values and the structure of the lowest 1^+ state, the two most collective 1^+ states from the "scissors"-mode region, and the γ vibrational state are presented in Table II. It is seen that in both regions there are quite collective 1^+ states.

The correlation between the collectivity of the 1^+_ν states and the Coriolis matrix elements (45) is demon-

TABLE II. Calculated excitation energies (MeV), reduced transition probabilities $B(E2,0^+0_{gr}\rightarrow 2^+K_\nu)$ (Wu), and main two-quasiparticle components of the $K^\pi_\nu=2^+_1$, 1^+_1, 1^+_{11}, and 1^+_{23} states.

K^π_ν / E_ν / $B(E2)\uparrow$	The main two-quasiparticle components	%	K^π_ν / E_ν / $B(E2)\uparrow$	The main two-quasiparticle components	%
2^+_1	nn523↓−521↓	30	1^+_{11}	nn532↓−521↓	20
0.786	pp411↑+411↓	28	3.66	pp402↑−411↑	16
22	nn523↑+521↓	16	1.3	nn514↓−512↑	16
	pp413↓−411↓	6		nn523↓−532↓	10
1^+_1	nn633↑−642↑	71	1^+_{23}	nn521↑−510↑	58
1.81	pp514↑−523↑	9	4.55	nn512↓−521↓	9
3.5	nn512↑−521↑	8	0.75	nn523↓−512↓	8
	nn624↑−633↑	2		pp411↑−420↑	5

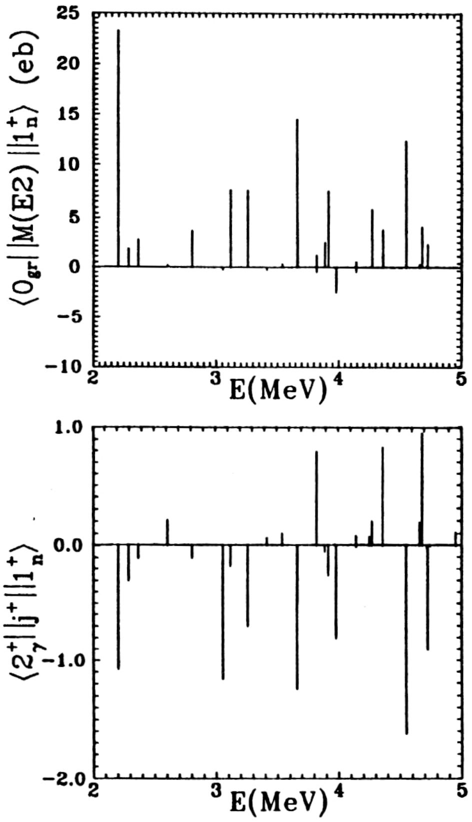

FIG. 2. The calculated reduced $E2$ matrix elements $\langle 0^+_{gr}\|M(E2)\|1^+_\nu\rangle$ and Coriolis-coupling matrix elements $\langle 2^+_\gamma\|j^+\|1^+_\nu\rangle$ in ^{166}Er.

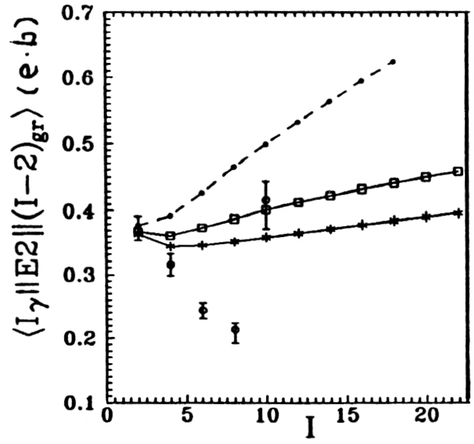

FIG. 3. The reduced $E2$ matrix elements for the $I_\gamma \rightarrow (I-2)_{gr}$ transitions in ^{166}Er: ○—experimental data; ●—adiabatic calculations; □—nonadiabatic calculations with $e_{\rm eff}=0.02$; *—nonadiabatic calculations with $e_{\rm eff}=0.3$ (see the text).

strated in Fig. 2. The larger the collectivity of the 1^+ band head, the stronger the Coriolis coupling between this band and the γ band. Indeed, this should be the case, since according to Eq. (45) the coupling occurs only if the 1^+ state and the γ vibrational state contain identical quasiparticles in their structures. This is most probable for the collective state, and Table II confirms this assertion. On the other hand, this correlation clearly shows the importance of the residual interaction for the description of the Coriolis coupling of 1^+_ν excitations to other states.

It should also be noted that the signs of the reduced $E2$ matrix elements $\langle 0^+_{gr}\|M(E2)\|1^+_\nu\rangle$ and of the Coriolis-coupling matrix elements $\langle 2^+_\gamma\|j^+\|1^+_\nu\rangle$ are mainly positive and negative, respectively, which means that the contribution of the 1^+_ν states to the matrix element of Eq. (45) is quite coherent. This favors the nonadiabatic effects caused by coupling to the 1^+_ν states.

The results of the microscopic calculations of the reduced $E2$ matrix elements for the $I_\gamma \rightarrow (I-2)_{gr}$ transitions in ^{166}Er as well as the experimental data[21] are shown in Fig. 3. The figure also includes calculations in the adiabatic approximation, i.e., without any Coriolis coupling. The microscopic calculations are performed with two values of the effective charge in the matrix element $M(E2)_{1^+}$:$e_{\rm eff}$ $=0.02$ and 0.3 [in the matrix elements $M(E2)_{Q_0}$ and $M(E2)_\gamma$ we keep $e_{\rm eff}=0.02$ in both cases]. The value $e_{\rm eff}=0.3$ was used to demonstrate the extremal case of very collective 1^+ states. As is seen from Fig. 3, the calculations do not reproduce the deep minimum in the experimental data. Thus, the conventional (without γ deformation) Coriolis interaction obtained within the familiar RPA cannot account for the nonadiabatic behavior. It is necessary to take into account other effects like γ deformation. The γ deformation results in a mixing of the ground and γ bands, and the corresponding enhancement of the Coriolis coupling should improve the description of the experimental data.[21] Such investigations are now in progress.

Since the main physical mechanism (Coriolis interaction) usually responsible for the $\Delta K=1$ coupling is suppressed for the ground and 1^+ bands, these two bands can be used to investigate more delicate effects (manifestation of γ deformation, etc.).

4. *E*1 TRANSITIONS IN ODD NUCLEI: INTERPLAY BETWEEN CORIOLIS INTERACTION AND COUPLING TO CORE VIBRATIONS

The broadest and most complete application of the model derived in Sec. 2 is for odd nuclei. In this section two expressive examples of competition between the Coriolis interaction and coupling to core vibrations are analyzed.

The $E1$ transitions between the members of the $5/2^-[532]$ rotational band and the members of the $5/2^+[413]$ and $3/2^+[411]$ bands in ^{153,155}Eu and ^{155,157}Tb are of special interest because they have strong fluctuations amounting to two orders of magnitude. The models taking into account only the pairing and the Coriolis mixing, e.g., the nonadiabatic rotational model (NRM),[39] fail in the description of these transitions. The deviation of the calculated $B(E1)$ values is up to two orders of magnitude from the experimental ones. The hindrance factors are $F \gg 1$ for $\Delta K=0$ transitions and $F \ll 1$ for $\Delta K=1$ transitions (see Fig. 4). As will be shown below, the use of the wave function (20) with quadrupole and octupole vibrational admixtures improves crucially the agreement with the experimental data.[18]

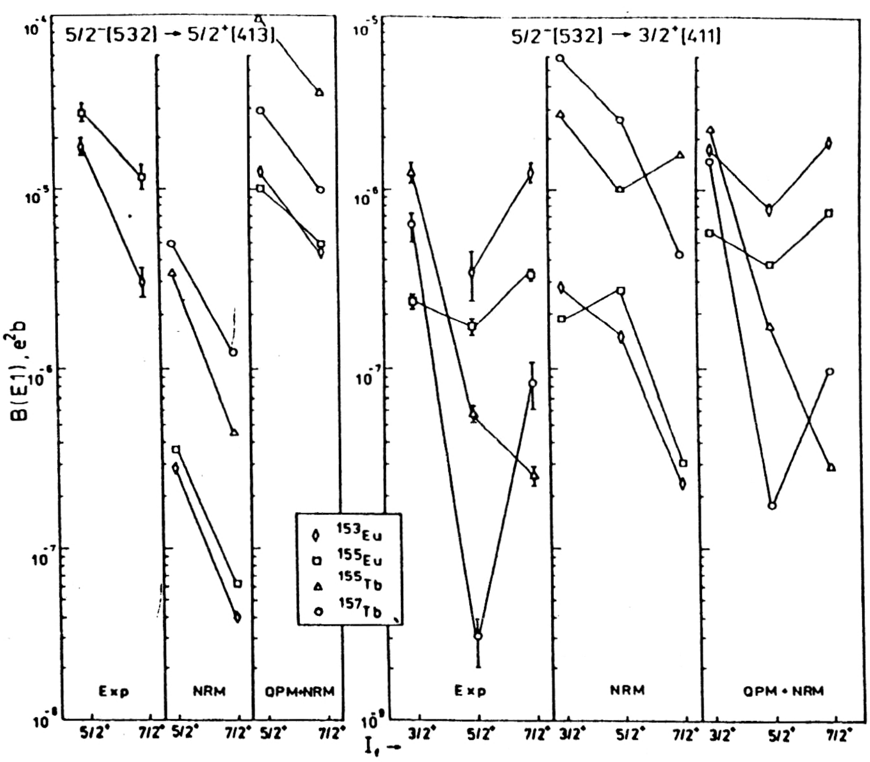

FIG. 4. The reduced probabilities of $E1$ transitions between the members of the $5/2^-[532]$ band and the $5/2^+[413]$ and $3/2^+[411]$ bands in ^{153,155}Eu and ^{155,157}Tb calculated within the NRM and the present model, labeled QPM +NRM.

The calculations have been performed according to the prescription of Sec. 2 but with the complicated version of the RPA, where the $K^\pi=1^-0$ and $K^\pi=1^-1$ one-phonon states are calculated with simultaneous use of the isoscalar octupole and isoscalar and isovector dipole forces, as well as with extraction of spurious admixtures caused by the violation of the transitional invariance of the Hamiltonian.[18,40]

The calculations have shown that the dominant contribution to the $E1$ transition matrix element for the odd nuclei comes (due to the octupole admixtures) from the $E1$ transition $0^+0_{gr}\rightarrow 1^-K_1$ in the even–even core. The influence on this transition of the "tail" of the giant dipole resonance (GDR) can be estimated by calculating the contribution to the $E1$ transition matrix element (34) of the q_1q_2 terms with energies $\varepsilon_1+\varepsilon_2$ from the GDR region. The contribution turns out to be 91–97% for both $\Delta K=0$ and 1.[40] Thus, just the "tail" of the GDR causes $0^+0_{gr}\rightarrow 1^-K_1$ transitions, whereas low-energy two-quasiparticle configurations mixed by octupole forces determine the main structure of the 1^-K_1 states.

In Table III the calculated energies and structure of low-lying nonrotational states in ^{153}Eu are presented. It is seen that the level energies are reproduced rather well. The main vibrational admixtures are, as a rule, of quadrupole character, whereas the octupole admixtures usually amount to several percent or less. The vibrational admixtures lead to a decrease of the amplitude of the main one-quasiparticle component and, as a result, to the attenuation of the Coriolis-mixing matrix elements. Table IV shows that just this effect can be the main reason for the Coriolis attenuation at low spins.

The results of our calculations for the $B(E2)$ values (labeled QPM+NRM) as compared with the results of the NRM and experimental data (see the references in Ref. 18) are shown in Fig. 4. It is seen that the NRM does not provide even a qualitative description of the $E1$ transitions. On the contrary, the QPM+NRM gives excellent agreement with the experimental data. It is remarkable that inclusion of the vibrational admixtures leads to more than an order-of-magnitude increase in the $\Delta K=0$ transitions and simultaneously provides a deep minimum in the $\Delta K=1$ transition in ^{157}Tb.

For an understanding of the results the different parts of the $E1$ transition matrix element (36) have been analyzed (see Table V and details in Ref. 18). It turns out that the $E1(\Delta K=0)$ transitions in the Eu nuclei are mainly between the principal K components of the initial and final states. These transitions are strongly enhanced by the coupling to the even–even core [see the $C\cdot D$ term in (36)]. On the other hand, in describing $E1(\Delta K=1)$ transitions in ^{157}Tb it is important to take into account not only the principal but also the small Coriolis-mixing components. Then both $\Delta K=1$ and $\Delta K=0$ terms will contribute to the total $E1(\Delta K=1)$ transition. Moreover, because of the large intrinsic matrix element the contribution to the total $E1(\Delta K=1)$ transition from the $\Delta K=0$ term turns out to be considerable. Because of the opposite signs of the $\Delta K=1$ and $\Delta K=0$ contributions to the total $E1(\Delta K=1)$ matrix element we have a mutual compensation, which explains the deep minimum in the ($BE1$, $\Delta K=1$) values for ^{157}Tb.

As can be seen from Table III the octupole admixtures in the wave functions are rather small. Thus, our calculations show that even small octupole admixtures in the wave functions of odd nuclei strongly influence $E1$ transitions and, in particular, can enhance the $B(E1)$ values by an order of magnitude. Earlier, similar results have been

TABLE III. The calculated energies and structure of low-lying nonrotational states in ^{153}Eu.

K^{π}	Energy, keV		Structure					
	Exp.	Calc.						
$5/2^+$	0	0	413↓	94%	411↓+Q_{221} 532↑+Q_{301}	3%, 0.1%	523↑+Q_{311} 541↑+Q_{311}	0.2% 0.03%
$5/2^-$	97	69	532↑	92%	411↑+Q_{311} 402↑+Q_{301}	0.8%, 0.3%	413↓+Q_{301}	0.1%
$3/2^+$	103	96	411↑	86%	411↓+Q_{221} 532↑+Q_{311}	6%, 0.6%	523↑+Q_{321} 541↑+Q_{301}	4%, 0.2%
$3/2^-$	637	448	541↑	84%	550↑+Q_{221} 422↓+Q_{301}	5%, 1%	420↑+Q_{311} 411↑+Q_{301}	1.7%, 0.4%
$7/2^-$	—	467	523↑	86%	411↑+Q_{321} 404↓+Q_{301}	9%, 0.4%	413↓+Q_{311}	0.4%
$1/2^-$	—	550	550↑	64%	532↑+Q_{321} 541↑+Q_{221}	10%, 8%	420↑+Q_{301}	9%
$1/2^+$	789	612	411↓	47%	411↑+Q_{221}	27%	413↓+Q_{221}	22%
$1/2^+$	635	645	420↑	76%	550↑+Q_{201} 532↑+Q_{321}	6%, 4%	422↓+Q_{221} 541↑+Q_{311}	5%, 2%
$5/2^-$	—	915	523↓	0.3%	532↑+Q_{201}	100%		
$5/2^+$	618	934	402↑	5%	413↓+Q_{201}	91%	532↑+Q_{301}	2.5%
$5/2^+$	707	1118	402↑	16%	532↑+Q_{301}	73%	413↓+Q_{201}	7%
$7/2^+$	570	1609	404↓	63%	523↑+Q_{301} 532↑+Q_{311}	21%, 4%	411↑+Q_{221}	7%

obtained for small quadrupole admixtures in the wave functions of odd nuclei.[12] It was shown that even very small quadrupole admixtures (about 1%) can dramatically influence $E2$ transitions in some odd nuclei.

It is clear that the large collectivity of octupole $K^{\pi}=0^-$ and 1^- states in the even–even core leads to large octupole admixtures in the wave functions of the corresponding odd nucleus and, as a result, to strong effects like the ones considered above. Nuclei at the onset of the rare-earth region have the most collective octupole low-lying states.[1,13,41] The nuclei considered above belong just to this group. But what will happen for heavier odd nuclei? Do octupole admixtures have much influence on $E1$ transitions in these nuclei also? In general, this does not seem to be the case, since for heavier nuclei the low-lying octupole states in the even–even cores are usually less collective. Also, some calculations for $E1$ transitions in odd nuclei of this sector show that often $E1$ transitions are satisfactorily described without taking into account octupole admixtures.[41] Nevertheless, we will demonstrate that in some cases the octupole admixtures play a crucial role in the description of $E1$ transitions for heavier nuclei as well.

Let us consider dipole $I_i^+ 9/2[624] \rightarrow I_f^- 7/2[514]$ transitions in ^{177}Hf, the data for which are given in Table VI. Numerous calculations are devoted to these transitions (see, for example, Refs. 25, 42, and 43), with the main purpose of explaining the extremely small experimental value of $B(E1, 9/2^+ \rightarrow 7/2^-)$. Though these calculations have not provided a good description of the experimental data, they have nevertheless shown that both the Coriolis interaction and octupole admixtures must be taken into account. Calculations[25,42,43] take into account the coupling

TABLE IV. Attenuation coefficients of the Coriolis matrix elements $(\alpha_{\rm fit}=\langle f|H_{\rm cor}|i\rangle_{\rm fit}/\langle f|H_{\rm cor}|i\rangle_{\rm QPM}, \alpha_{\rm QPM}=C^{\nu_i}_{q_i}C^{\nu_f}_{q_f})$.

$f \quad i$	^{153}Eu		^{155}Eu		^{155}Tb		^{157}Tb	
	$\alpha_{\rm fit}$	$\alpha_{\rm QPM}$	$\alpha_{\rm fit}$	$\alpha_{\rm QPM}$	$\alpha_{\rm fit}$	$\alpha_{\rm QPM}$	$\alpha_{\rm fit}$	$\alpha_{\rm QPM}$
523↑—532↑	0.7	0.9	0.8	0.9	0.7	0.9	0.8	0.9
532↑—541↑	0.6	0.9	0.6	0.9	0.6	0.9	0.7	0.9
541↑—550↑	0.8	0.7	0.7	0.7	0.8	0.7	0.8	0.6
404↓—413↓	0.8	0.9	0.8	0.9	0.8	0.9	0.8	0.9
402↑—411↑	0.4	0.4	0.5	0.7	0.7	0.8	0.6	0.7
411↑—420↑	0.5	0.8	0.6	0.7	0.9	0.8	0.8	0.8

TABLE V. Structure of the reduced $E1$ matrix elements $M(E1,I_i^{\pi_i}\to I_f^{\pi_f}) = \langle I_f^{\pi_f}\|E1\|I_i^{\pi_i}\rangle/\sqrt{2I_i+1}$ [see Eq. (32)] between members of the 5/2⁻[532] band and the 5/2⁺[413] and 3/2⁺[411] bands in ^{153}Eu and ^{151}Tb. Here $M_{fi}(E1) = (\Psi_f(K_f^{\pi_f})\hat{M}(E1,\mu = K_f \pm K_i)\Psi_i(K_i^{\pi_i}))$, $F=B(E1)_{\rm exp}/B(E1)_{\rm QPM+NRM}$, $a_{if}=b^{I_f}_{K_f\nu_f}b^{I_i}_{K_i\nu_i}(I_i\pm K_i 1\mu|I_fK_f)$.

^{153}Eu, $I_i^{\pi_i}$5/2[532] → $I_f^{\pi_f}$5/2[413], $\Delta K=0$								
$I_i^{\pi_i}\to I_f^{\pi_f}$			$5/2^-\to 5/2^+$		$5/2^-\to 7/2^+$		$11/2^-\to 9/2^+$	
f — i	ΔK	$M_{fi}(E1)$ 10^{-2} e·fm	a_{if}	$a_{if}M_{fi}(E1)$ 10^{-2} e·fm	a_{if}	$a_{if}M_{fi}(E1)$ 10^{-2} e·fm	a_{if}	$a_{if}M_{fi}(E1)$ 10^{-2} e·fm
404↓—523↑	0	−27.4	—	—	—	—	−0.031	0.84
413↓—523↑	1	1.5	—	—	—	—	0.199	0.30
413↓—532↑	0	−4.4	0.832	−3.68	0.519	−2.29	−0.521	2.30
413↓—541↑	1	0.6	−0.083	0.04	0.130	−0.06	0.097	−0.05
402↑—532↑	0	71.0	0.002	0.14	0.005	0.31	−0.0010	−0.58
411↑—532↑	1	−2.4	0.034	−0.08	0.020	−0.05	0.066	−0.16
411↑—541↑	0	−7.4	0.005	−0.04	0.010	−0.07	−0.024	0.18
$M(E1, I_i^{\pi_i}\to I_f^{\pi_f})$			$-3.62\cdot10^{-2}$ e·fm		$-2.62\cdot10^{-2}$ e·fm		$3.84\cdot10^{-2}$ e·fm	
$B(E1, I_i^{\pi_i}\to I_f^{\pi_f})_{\rm exp}$			$1.8(2)\cdot10^{-5}$ e^{2}b		$3.0(6)\cdot10^{-6}$ e^{2}b		$8.0(14)\cdot10^{-6}$ e^{2}b	
F			0.7		2.6		1.0	
^{157}Tb, $I_i^{\pi_i}$5/2[532] → $I_f^{\pi_f}$3/2[411], $\Delta K=1$								
$I_i^{\pi_i}\to I_f^{\pi_f}$			$5/2^-\to 3/2^+$		$5/2^-\to 5/2^+$		$5/2^-\to 7/2^+$	
f — i	ΔK	$M_{fi}(E1)$ 10^{-2} e·fm	a_{if}	$a_{if}M_{fi}(E1)$ 10^{-2} e·fm	a_{if}	$a_{if}M_{fi}(E1)$ 10^{-2} e·fm	a_{if}	$a_{if}M_{fi}(E1)$ 10^{-2} e·fm
413↓—532↑	0	6.4	—	—	0.038	0.24	0.037	0.24
402↑—532↑	0	13.0	—	—	0.026	0.33	0.025	0.32
411↑—532↑	1	0.6	0.813	0.47	0.531	0.31	0.216	0.13
411↑—541↑	0	−17.4	−0.044	0.77	0.043	−0.75	0.059	−1.02
420↑—541↑	1	3.7	0.002	0.01	0.003	0.01	0.002	0.01
$M(E1, I_i^{\pi_i}\to I_f^{\pi_f})$			$1.25\cdot10^{-2}$ e·fm		$0.14\cdot10^{-2}$ e·fm		$-0.32\cdot10^{-2}$ e·fm	
$B(E1, I_i^{\pi_i}\to I_f^{\pi_f})_{\rm exp}$			$6.1(12)\cdot10^{-7}$ e^{2}b		$3.1(13)\cdot10^{-9}$ e^{2}b		$8.4(24)\cdot10^{-8}$ e^{2}b	
F			2.5		5.9		1.2	

to octupole core vibrations. Nevertheless, they have serious shortcomings: 1) the octupole phonons are included in a phenomenological way; 2) the calculations for $E1$ transitions are not followed for a description of the low-energy spectrum in ^{177}Hf.

More realistic microscopic calculations have been performed recently[19] within the model given in Sec. 2. The calculations of $B(E1)$ values have been made with three prescriptions: with the Coriolis interaction only (a), with both the Coriolis interaction and coupling to core quadrupole and octupole vibrations (b), and with an improved version of (b) in which the $E1$ matrix elements L_g^{E1} for the even–even core were calculated with allowance for the "tail" of the GDR (c).

The results are presented in Tables VI and VII. It is seen that they are in quite satisfactory agreement with experimental data for both the energy spectrum and the $B(E1)$ values. The most important result is that inclusion of octupole admixtures dramatically improves the description of the $B(E1,9/2^+\to7/2^-)$ value as compared with the case in which only the Coriolis coupling is taken into account. Simultaneously, the description of the other transitions remains quite appropriate.

Thus, our calculations show that the most correct way of describing $E1$ transitions in rare-earth odd nuclei is simultaneous use of the Coriolis interaction and coupling to even–even core vibrations. It is the interplay of these two interactions that leads to the anomalous behavior of the $E1$ transitions. The microscopic scheme presented in Sec. 2 provides a satisfactory description of both the electric transitions and the low-energy spectrum. Moreover, in the framework of this scheme the calculations for odd nuclei are consistent with calculations for neighboring even–even nuclei.

5. STRUCTURE OF LOW-LYING STATES IN ODD–ODD ^{166}Ho

The results presented here[9] represent the first systematic application of the model described in Sec. 2 to odd–

TABLE VI. Energies and structure of low-lying states in ^{177}Hf.

K^π	Energy, keV			Structure, %			
	exp.	IQM*	QPM				
7/2⁻	0	0	0	514↓	97.3	512↓+Q_{221}	2.1
9/2⁺	321.3	294	353	624↑	98.8		
5/2⁻	508.1	711	542	512↑	95.5	510↑+Q_{221}	2.1
5/2⁻	—	1994	1542	523↓	9.5	512↑+Q_{201} 521↑+Q_{221}	83.1 7.0
1/2⁻	559.4	783	585	521↓ 510↑	-83.1 5.4	523↓+Q_{221} 521↑+Q_{221}	2.7 4.1
1/2⁻	(567)	1111	604	510↑ 521↓	71.6 7.3	512↓+Q_{221} 512↑+Q_{221}	12.1 7.0
7/2⁺	745.9	801	796	633↑	95.7	651↑+Q_{221}	2.5
3/2⁻	805.7	1486	780	512↓	66.2	510↑+Q_{221} 514↓+Q_{221}	16.2 14.7
3/2⁻	(1502)	2066	1284	521↑	42.0	521↓+Q_{221} 633↑+Q_{321}	41.2 14.4
5/2⁺	—	1132	951	642↑	89.4	660↑+Q_{221} 624↑+Q_{221}	5.5 1.3
7/2⁻	1057.8	1883	1213	503↑	22.2	514↓+Q_{201} 501↑+Q_{221}	74.2 2.2
7/2⁻	—		1457	503↑	61.9	514↓+Q_{201} 501↑+Q_{221}	25.8 7.0
3/2⁻	1434	3673	1536	501↑	52.7	503↑+Q_{221} 514↓+Q_{221}	23.3 15.2

*Energies calculated within the Independent-Quasiparticle Model.

odd nuclei. At this first stage only the coupling to core vibrations is taken into account. Calculations with the Coriolis interaction are in progress and will be presented later. The calculations presented here have been performed for the states with excitation energy up to 0.5 MeV in the isotopes $^{160-168}$Ho. The results of systematic microscopic calculations within the same model for neighboring odd and even nuclei can be found in Refs. 14, 20, and 13, respectively. For the sake of brevity we present here only the results for ^{166}Ho. Details of the calculations are given in Ref. 9.

The calculated energies and structure of the nonrotational states in ^{166}Ho are presented in Table VIII. For each level two theoretical values are given: $E'_{\rm th} = \eta_{\nu\gamma} - \eta_{\nu_0\gamma_0}$ and

TABLE VII. Hindrance factors $F=B(E1)_{\rm exp}/B(E1)_{\rm theor}$ for $E1$ transitions $I_i^+ 9/2[624] \to I_f^- 7/2[514]$ in ^{177}Hf (see comments in the text).

ΔJ	$J_i^\pi \to J_f^\pi$	E_γ, keV	$B(E1)_{\rm exp}$, 10^{-7} e²b	F		
				a	b	c
−1	21/2⁺ → 19/2⁻	283.4	9.32(29)	0.73	2.42	0.89
	19/2⁺ → 17/2⁻	292.5	7.46(27)	0.74	2.59	0.91
	17/2⁺ → 15/2⁻	291.4	6.06(9)	0.68	2.56	0.86
	15/2⁺ → 13/2⁻	299.0	3.93(25)	0.66	2.77	0.92
	13/2⁺ → 11/2⁻	305.5	1.79(3)	0.65	3.48	1.12
	11/2⁺ → 9/2⁻	313.7	0.495(66)	0.27	3.78	1.16
	9/2⁺ → 7/2⁻	321.3	0.0393(39)	10.3	1.40	0.88
0	19/2⁺ → 19/2⁻	69.2	7,67(20)	1.03	2.82	0.19
	17/2⁺ → 17/2⁻	88.4	8,32(10)	1.06	2.85	0.30
	15/2⁺ → 15/2⁻	117.2	9.58(10)	1.00	2.67	0.38
	13/2⁺ → 13/2⁻	145.8	9.16(7)	1.11	2.92	0.54
	11/2⁺ → 11/2⁻	177.0	9.11(57)	1.10	2.86	0.66
	9/2⁺ → 9/2⁻	208.3	6.74(38)	1.15	2.98	0.82
+1	9/2⁺ → 11/2⁻	71.7	2.44(23)	1.52	4.10	1.92

$E_{\text{th}} = \eta_{\nu\gamma} - \eta_{\nu_0\gamma_0} + (h^2/2J)(I^2 - K^2_{I=K}) - (h^2/2J)(I^2 - K^2_{I=K_0})$. It is seen that the model provides a satisfactory description of the energy spectrum (together with the spectrum of the neighboring odd nuclei; see Ref. 20). The most interesting result of the calculations is the existence in low-lying states of rather large vibrational admixtures. The simple estimates (like those for odd nuclei in Ref. 12) with use of the amplitudes of components of the states from Table VIII show that these vibrational admixtures strongly influence the $E2$ and $E1$ transitions. We have quite the same situation as in odd nuclei. This is not surprising, since the matrix elements of $E\lambda$ transitions in odd and odd–odd nuclei have similar structures [see (36) and (37)].

The calculations for Ho isotopes show that the main strength of the γ vibrations built on the ground-state configurations is concentrated in intrinsic states with excitation energies above 1 MeV. An exception to this general rule is the 2^- (525 keV) state in ^{166}Ho, which has 26% of the γ vibrational component. Recently, a 2^- γ vibrational band was suggested[44] in ^{166}Ho with a band head at 543 keV, which is in rather nice agreement with our calculations. It is interesting that up to the present there is no conclusive experimental evidence for the calculated 5^- (260 keV) state.

The mixing of the neutron–proton configurations with the same K^π should be noted. The mixing is caused by the quasiparticle–phonon interaction. Such mixing (do not confuse this with Coriolis mixing) is well known in odd nuclei but has not been calculated before in odd–odd nuclei. This effect can be very important for the study of the structure of low-lying states in odd–odd nuclei. For example, it is the admixture of the spin-flip configuration $1^+\{\pi7/2[523],\nu5/2[523]\}$ to the low-lying states in odd–odd ^{166,168}Ho that explains the low experimental values of log ft in these nuclei.[9] The results of corresponding calculations are presented in Table IX.

6. CONCLUSIONS

An extension of the Quasiparticle–Phonon Model has been proposed by taking into account the rotation–vibration coupling in even–even, odd, and odd–odd nuclei. This extension is an important step in the derivation of a general microscopic model for the description of vibrational and rotational degrees of freedom in strictly deformed nuclei on the same microscopic footing. Three examples of calculations for even–even, odd, and odd–odd nuclei have been considered.

1) In ^{166}Er the Coriolis interaction between the ground and γ bands through low-lying 1^+ states (together with the "scissors" mode) has been analyzed as a possible origin of the nonadiabatic effects in $E2(\gamma\rightarrow gr)$ transitions.[24] It has been shown that the Coriolis coupling between the ground and 1^+ bands is absent within the RPA for axially deformed nuclei. This is a rather unexpected result of general character, which was not mentioned before in spite of intensive investigation of the "scissors" mode. Therefore, the Coriolis coupling can exist and lead to the nonadiabatic effects in ^{166}Er only under some special conditions, for example, if a triaxiality of this nucleus occurs. The contribution of the "scissors" mode to the nonadiabatic effects in $E2(\gamma\rightarrow gr)$ transitions can be much more noticeable in nuclei like ^{172}Yb. Because of a small collectivity of the γ-vibrational state in such nuclei, the direct $E2$ transition ($2^+_\gamma \rightarrow 0^+_{gr}$) is weak and, as a result, the effects of indirect (due to the Coriolis interaction) $E2$ transitions should be larger.

2) The strong influence of small octupole vibrational admixtures in the wave functions of odd nuclei on the $E1$ transitions in Eu–Tb isotopes and in ^{177}Hf was shown in Refs. 18 and 19. It was demonstrated that the anomalous behavior of $E1$ transitions in these nuclei can be explained by the competition between the quasiparticle–phonon and Coriolis-interaction effects. It should be noted that the model provides the possibility for simultaneous description of the electric transition and the energy spectrum in odd nuclei.

3) In low-lying states of odd–odd ^{166}Ho rather large vibrational admixtures are predicted as well as the mixing of neutron–proton configurations due to the quasiparticle–phonon interaction. Both effects are quite important for the study of level structure, $E1$ and $E2$ transitions, and β transitions in odd–odd nuclei.

7. APPENDIX

In Sec. 2.1 the following functions characterizing the RPA phonons are used:

$$\psi^g_{q_1q_2} = \sqrt{\frac{1+\delta_{\mu,0}}{2\tilde{Y}^g_\tau}}\,\frac{f^{\lambda\mu}_{q_1q_2}u^{(+)}_{q_1q_2}}{\varepsilon_{q_1q_2}-\omega_g}, \tag{61}$$

$$\varphi^g_{q_1q_2} = \sqrt{\frac{1+\delta_{\mu,0}}{2\tilde{Y}^g_\tau}}\,\frac{f^{\lambda\mu}_{q_1q_2}u^{(+)}_{q_1q_2}}{\varepsilon_{q_1q_2}+\omega_g}, \tag{62}$$

$$X^g_\tau = (1+\delta_{\mu,0})\sum_{q_1q_2\in\tau}\frac{(f^{\lambda\mu}_{q_1q_2}u^{(+)}_{q_1q_2})^2\varepsilon_{q_1q_2}}{\varepsilon^2_{q_1q_2}+\omega^2_g}, \tag{63}$$

$$\tilde{Y}^g_\tau = Y^g_\tau + Y^g_{-\tau}\left\{\frac{1-(\kappa_0^{(\lambda\mu)}+\kappa_1^{(\lambda\mu)})X^g_\tau}{(\kappa_0^{(\lambda\mu)}-\kappa_1^{(\lambda\mu)})X^g_{-\tau}}\right\}^2, \tag{64}$$

where

$$Y^g_\tau = (1+\delta_{\mu,0})\sum_{q_1q_2\in\tau}\frac{(f^{\lambda\mu}_{q_1q_2}u^{(+)}_{q_1q_2})^2\varepsilon_{q_1q_2}\omega_g}{(\varepsilon^2_{q_1q_2}+\omega^2_g)^2} \tag{65}$$

and the secular equation for determining the one-phonon energies ω_g is

$$1-(\kappa_0^{(\lambda\mu)}+\kappa_1^{(\lambda\mu)})(X^g_\tau+X^g_{-\tau})+4\kappa_0^{(\lambda\mu)}\kappa_1^{(\lambda\mu)}X^g_\tau X^g_{-\tau}=0. \tag{66}$$

Here, $\varepsilon_{q_1q_2} = \varepsilon_{q_1} + \varepsilon_{q_2}$. For $\lambda\mu=20$ the expressions (61)–(66) are more complicated, since in this case the interaction in the particle–particle channel is embraced to extract the spurious admixtures connected with particle-number nonconservation. The corresponding expressions can be found in Refs. 1, 2, and 10.

TABLE VIII. The level energies and structure of low-lying states in ^{166}Ho.

K^π	Structure	%	E_{exp} / E'_{Th} / E_{Th} (keV)	K^π	Structure	%	E_{exp} / E'_{Th} / E_{Th} (keV)
0^-	7/2 523−7/2 633	89%	0	7^-	7/2 523+7/2 633	79%	6
	7/2 523−3/2 651−Q^+_{22}	10%	0		7/2 523+3/2 651+Q^+_{22}	11%	−45
			0		3/2 541+7/2 633+Q^+_{22}	5%	18
					7/2 523+11/2 615−Q^+_{22}	3%	
5^-	7/2 523+3/2 651	81%	—	2^-	7/2 523−3/2 651	66%	(543)
	3/2 541+7/2 633	12%	215		3/2 541−7/2 633	5%	507
	7/2 523+7/2 633−Q^+_{22}	6%	260		7/2 523−7/2 633±Q^+_{22}	26%	525
					7/2 523−1/2 660−Q^+_{22}	7%	
3^+	7/2 523−1/2 521	92%	191	4^+	7/2 523+1/2 521	92%	372
	3/2 541−1/2 521+Q^+_{22}	4%	178		3/2 541+1/2 521+Q^+_{22}	4%	222
	3/2 411−1/2 521+Q^+_{32}	2%	205		3/2 411+1/2 521+Q^+_{32}	2%	258
6^+	7/2 523+5/2 512	82%	295	1^+	7/2 523−5/2 512	80%	426
	7/2 523+5/2 523	3%	263		7/2 523−5/2 523	18%	411
	7/2 523+9/2 624−Q^+_{32}	5%	317		7/2 523−9/2 624+Q^+_{32}	1%	420
	7/2 523+1/2 660+Q^+_{32}	2%			7/2 523−1/2 660−Q^+_{32}	1%	
	7/2 523+1/2 400+Q^+_{32}	2%			7/2 523−1/2 400−Q^+_{32}	1%	
1^-	3/2 411−1/2 521	95%	351	2^-	3/2 411+1/2 521	94%	563
	3/2 411−5/2 642+Q^+_{32}	1%	354		7/2 523+1/2 521−Q^+_{32}	2.5%	526
	3/2 411+3/2 651−Q^+_{32}	1%	363		3/2 541+1/2 521+Q^+_{30}	1%	544
	5/2 523+1/2 521−Q^+_{32}	1%					
	3/2 541−1/2 521+Q^+_{30}	1%					
0^-	1/2 411−1/2 521	96%	525	1^-	1/2 411+1/2 521	96%	373
	1/2 411+3/2 521−Q^+_{22}	2%	560		1/2 411−3/2 521+Q^+_{22}	2%	381
	3/2 411+1/2 521−Q^+_{22}	1%	560		3/2 411−1/2 521−Q^+_{22}	1%	390
5^+	7/2 523+3/2 521	70%	264	2^+	7/2 523−3/2 521	79%	430
	3/2 411+7/2 633	21%	259		3/2 411−7/2 633	1%	409
	7/2 523+7/2 633−Q^+_{32}	5%	304		7/2 523−7/2 514+Q^+_{22}	6%	427
	7/2 532+7/2 514−Q^+_{22}	3%			7/2 523−7/2 633+Q^+_{32}	5%	
					7/2 523+1/2 521−Q^+_{22}	2%	
1^+	7/2 523−5/2 523	71%	567	6+	7/2 523+5/2 523	72%	—
	7/2 523−5/2 512	13%	554		7/2 523+5/2 512	11%	660
	7/2 523−9/2 624−Q^+_{32}	4%	563		7/2 523+9/2 624−Q^+_{32}	5%	714
	3/2 541−5/2 523+Q^+_{22}	3%			3/2 541+5/2 523+Q^+_{22}	3%	
	7/2 523−1/2 530−Q^+_{22}	2%			7/2 523+1/2 651−Q^+_{32}	2%	
	7/2 523−1/2 651−Q^+_{32}	2%			7/2 523+1/2 530+Q^+_{22}	2%	
2^+	3/2 411−7/2 633	82%	—	5^+	3/2 411+7/2 633	82%	—
	7/2 523−3/2 521	14%	646		7/2 523+3/2 521	13%	608
	3/2 411−3/2 651+Q^+_{22}	4%	664		3/2 411+3/2 651+Q^+_{22}	5%	653
0^+	7/2 404−7/2 633	75%	803	7^+	7/2 404+7/2 633	75%	915
	7/2 404−3/2 651−Q^+_{22}	14%	839		7/2 404+3/2 651+Q^+_{22}	14%	915
	7/2 404−11/2 505−Q^+_{32}	4%	839		7/2 404+11/2 505−Q^+_{32}	3.5%	975
	3/2 402−7/2 633−Q^+_{22}	3%			3/2 402+7/2 633+Q^+_{22}	3%	
2^-	3/2 541−7/2 633	70%	—	5^-	3/2 541+7/2 633	73%	—
	7/2 523−7/2 633+Q^+_{22}	10%	708		7/2 523+7/2 633−Q^+_{22}	9%	815
	1/2 550−7/2 633−Q^+_{22}	8%	726		1/2 550−7/2 633−Q^+_{22}	7%	860
	3/2 541−3/2 651+Q^+_{22}	5%			3/2 541+3/2 651+Q^+_{22}	5%	
2^-	7/2 523−11/2 615	78%	—	9^-	7/2 523+11/2 615	77%	—
	7/2 523−7/2 633+Q^+_{22}	12%	1131		7/2 523+7/2 633+Q^+_{22}	14%	1082
	7/2 523−7/2 504+Q^+_{32}	6%	1149		7/2 523+7/2 504+Q^+_{32}	9%	1154

TABLE IX. The log ft of β_- transitions leading to the low-lying 1^+ states in odd–odd ^{166,168}Ho isotopes.

Daughter nucleus	Final level E [keV], I^π	$\lvert C^{1+}_{\pi 7/2[523],\nu 5/2[523]}\rvert^2$	log ft Theory	log ft Experiment
^{166}Ho	426.0(1^+)	0.18	4.96	5.12
^{168}Ho	192.5(1^+)	0.02	5.86	5.50
^{168}Ho	630.4(1^+)	0.66	4.34	4.60

The functions $\Gamma^{\rm ph}_{gq_1q_2}(\tau)$, $\Gamma^{\rm pair(+)}_{iq_1q_2}(\tau)$, and $\Gamma^{BB}_{\lambda\mu q_1q_2q_1'q_2'}(\tau)$ involved in (11)–(13) have the form

$$\Gamma^{\rm ph}_{gq_1q_2}(\tau)=\sqrt{\frac{2}{\tilde{Y}^g_\tau}}\, f^{\lambda\mu}_{q_1q_2}v^{(-)}_{q_1q_2}, \tag{67}$$

$$\Gamma^{\rm pair(+)}_{iq_1q_2}(\tau)=1/\sqrt{2}G_\tau u_{q_1}v_{q_1}(u^2_{q_2}-v^2_{q_2})\psi^{20i}_{q_1q_2}, \tag{68}$$

$$\Gamma^{\rm pair(-)}_{iq_1q_2}(\tau)=1/\sqrt{2}G_\tau u_{q_1}v_{q_1}(u^2_{q_2}-v^2_{q_2})\varphi^{20i}_{q_1q_2}, \tag{69}$$

and

$$\Gamma^{BB}_{\lambda\mu q_1q_2q_1'q_2'}(\tau)=f^{\lambda\mu}_{q_1q_2}f^{\lambda\mu}_{q_1'q_2'}v^{(-)}_{q_1q_2}v^{(-)}_{q_1'q_2'}. \tag{70}$$

Further,

$$\Gamma_{gq_1q_2}(\tau)=\sqrt{\frac{2}{\tilde{Y}^g_\tau(1+\delta_{K,0}(1-\delta_{\mu,0}))}}\,\tilde{f}^{\lambda\mu}_{q_1q_2}v^{(-)}_{q_1q_2}$$

$$-\delta_{q_1q_2}\delta_{\lambda\mu,20}\sqrt{2}G_\tau u_{q_1}v_{q_1}\times\sum_{q\in\tau}(u^2_q-v^2_q)\sum_i(\psi^{20i}_{qq}+\phi^{20i}_{qq}), \tag{71}$$

where for the operator of electric type $\hat{f}^{\lambda\mu}$ we have

$$\tilde{f}^{\lambda\mu}_{q_1q_2}=\langle\tilde{q}_1|\hat{f}^{\lambda\mu}|\tilde{q}_2\rangle(\delta_{\sigma_1,\sigma_2}-\sigma_1\delta_{\sigma_1,-\sigma_2}) \tag{72}$$

(the same expression holds for $\tilde{p}^{\lambda\mu}_{q_1q_2}$) and for the operator of magnetic type $\hat{j}^+$ we have

$$\tilde{j}^+_{q_1q_2}=\langle\tilde{q}_1|\hat{j}^+|\tilde{q}_2\rangle(\sigma_1\delta_{\sigma_1,\sigma_2}+\delta_{\sigma_1,-\sigma_2}). \tag{73}$$

The coefficient $k^{CC}_{\gamma\gamma'}$ from (37) is equal to 1 except for the cases

$$k^{CC}_{\gamma\gamma'}=\begin{pmatrix}\frac{1}{\sqrt{2}}(\delta_{\sigma_s,+1}\delta_{\sigma_r,-1}-\gamma\delta_{\sigma_s,-1}\delta_{\sigma_r,+1}) & \text{for } K=0, & K'\neq 0\\ \frac{1}{\sqrt{2}}(\delta_{\sigma_{s'},+1}\delta_{\sigma_{r'},-1}-\gamma'\delta_{\sigma_{s'},-1}\delta_{\sigma_{r'},+1}) & \text{for } K\neq 0, & K'=0\end{pmatrix}, \tag{74}$$

and the coefficient $k^{DD}_{\gamma_q\gamma'_1}$ is equal to $k^{K'}_\mu k^K_\mu(1+\delta_{K,0}\delta_{K',0}(1-\delta_{\mu,0}))$ except for the cases

$$k^{DD}_{\gamma\gamma'}=\begin{pmatrix}\frac{1}{\sqrt{2}k^{K'}_\mu}(\delta_{\sigma_s,+1}\delta_{\sigma_r,-1}-\gamma\delta_{\sigma_s,-1}\delta_{\sigma_r,+1}) & \text{for } K=0, & K'\neq 0\\ \frac{1}{\sqrt{2}k^{K}_\mu}(\delta_{\sigma_{s'},+1}\delta_{\sigma_{r'},-1}-\gamma'\delta_{\sigma_{s'},-1}\delta_{\sigma_{r'},+1}) & \text{for } K\neq 0, & K'=0\end{pmatrix}. \tag{75}$$

The author is grateful to Profs. V. G. Soloviev, I. N. Mikhailov, V. M. Mikhailov, R. Sheline, Drs. N. A. Bonch–Osmolovskaya, B. A. Alikov, C. Fahlander, J. Kvasil, R. Kulessa, R. Nazmitdinov, P. N. Usmanov, and A. A. Okhunov for fruitful discussions, collaboration, and help.

[1] V. G. Soloviev, *Theory of Complex Nuclei* (Pergamon Press, Oxford, 1976) [Russ. original, Nauka, Moscow, 1971].
[2] V. G. Solov'ev, *Theory of Atomic Nuclei (Quasiparticles and Phonons)* (Institute of Physics, Bristol, England, 1992) [Russ. original, Énergoatomizdat, Moscow, 1989].
[3] V. G. Soloviev, V. O. Nesterenko, and S. I. Bastrukov, Z. Phys. A **309**, 353 (1983).
[4] V. G. Soloviev, Phys. Lett. **21**, 320 (1966).
[5] J. P. Boisson, R. Peipenbring, and W. Ogle, Phys. Rep. **26**, 99 (1976).
[6] V. Paar, Nucl. Phys. **A331**, 16 (1979).
[7] L. Bennour, J. Libert, V. Meyer, and P. Quentin, Nucl. Phys. **A465**, 35 (1987).
[8] J. Kvasil, V. O. Nesterenko, and I. Hrivnacova, Czech. J. Phys. **41**, 345 (1991).
[9] J. Kvasil, R. K. Sheline, V. O. Nesterenko, I. Hrivnacova, and D. Nosek, Z. Phys. A **343**, 145 (1992).
[10] V. O. Nesterenko, V. G. Soloviev, and A. V. Sushkov, Preprint P4-86-115, JINR, Dubna (1986).
[11] V. G. Soloviev, Z. Phys. A **334**, 143 (1989).
[12] S. I. Bastrukov and V. O. Nesterenko, in *Proc. of the Intern. Symposium on In-Beam Nuclear Spectroscopy* (Debrecen, Hungary, 1984), p. 689.

[13] E. P. Grigorjev and V. G. Soloviev, *Structure of Even Deformed Nuclei* (Nauka, Moscow, 1974).
[14] F. A. Gareev, S. P. Ivanova, V. G. Soloviev, and S. I. Fedotov, Fiz. Elem. Chastits At. Yadra **4**, 357 (1973) [Sov. J. Part. Nucl. **4**, 148 (1973)].
[15] S. P. Ivanova, A. L. Komov, L. A. Malov, and V. G. Solov'ev, Izv. Akad. Nauk SSSR, Ser. Fiz. **37**, 911 (1973); **39**, 1612 (1975).
[16] F. A. Gareev, S. P. Ivanova, V. G. Soloviev, and S. I. Fedotov, Nucl. Phys. **A171**, 134 (1971).
[17] N. A. Bonch-Osmolovskaya, V. A. Morozov, and V. O. Nesterenko, Izv. Akad. Nauk SSSR, Ser. Fiz. **49**, 843 (1985).
[18] B. A. Alikov, Kh. N. Badalov, V. O. Nesterenko, A. V. Sushkov, and J. Wawryszczuk, Z. Phys. A **331**, 265 (1988).
[19] B. A. Alikov, N. A. Bonch-Osmolovskaya, and V. O. Nesterenko, Izv. Ross. Akad. Nauk, Ser. Fiz. **56**, No. 11, 43 (1992).
[20] N. A. Bonch-Osmolovskaya and V. O. Nesterenko, Izv. Ross. Akad. Nauk, Ser. Fiz. **56**, No. 11, 53 (1992).
[21] C. Fahlander, B. Varnesting, A. Backlin, *et al.*, Nucl. Phys. **A537**, 183 (1992).
[22] I. N. Mikhailov and Ph. N. Usmanov, Ann. Phys. **2**, 239 (1993).
[23] N. Lo Iudice and F. Palumbo, Phys. Rev. Lett. **41**, 1532 (1978).
[24] V. O. Nesterenko, Ph. N. Usmanov, A. A. Okhunov, and C. Fahlander, J. Phys. G **19**, 1339 (1993).
[25] A. Bohr and B. R. Mottelson, *Nuclear Structure*, Vol. 2 (Benjamin, New York, 1974).
[26] V. G. Soloviev and N. Yu. Shirikova, Z. Phys. A **301**, 263 (1981).
[27] V. O. Nesterenko, Z. Phys. A **335**, 147 (1990).
[28] V. O. Nesterenko, V. G. Solov'ev, A. V. Sushkov, and N. Yu. Shirikova, Yad. Fiz. **44**, 1443 (1986) [Sov. J. Nucl. Phys. **44**, 938 (1986)].
[29] R. Nojarov and A. Faessler, Nucl. Phys. **A484**, 1 (1988).
[30] C. De Coster and K. Heyde, Nucl. Phys. **A524**, 441 (1991).
[31] J. Kvasil, I. N. Mikhailov, R. Ch. Safarov, and B. Choriev, Czech. J. Phys. **B29**, 843 (1979).
[32] A. S. Davydov and G. F. Filippov, Nucl. Phys. **8**, 237 (1958).
[33] A. Faessler, W. Greiner, and R. K. Sheline, Nucl. Phys. **70**, 33 (1965).
[34] A. Arima and F. Iachello, Adv. Nucl. Phys. **13**, 139 (1984).
[35] I. N. Mikhaĭlov and P. N. Usmanov, Yad. Fiz. **54**, 1239 (1991) [Sov. J. Nucl. Phys. **54**, 753 (1991)].
[36] A. Faessler, R. Nojarov, and F. G. Scholtz, Nucl. Phys. **A515**, 237 (1990).
[37] M. I. Baznat and N. I. Pyatov, Yad. Fiz. **21**, 708 (1975) [Sov. J. Nucl. Phys. **21**, 365 (1975)].
[38] C. Magnusson, Phys. Scr. **43**, 460 (1991).
[39] M. I. Baznat, N. I. Pyatov, and M. I. Chernei, Fiz. Elem. Chastits At. Yadra **4**, 941 (1973) [Sov. J. Part. Nucl. **4**, 384 (1974)].
[40] B. A. Alikov, Kh. N. Badalov, V. O. Nesterenko, A. V. Sushkov, and J. Wawryszczuk, Preprint E4-87-917, JINR, Dubna (1987).
[41] V. Andreĭchev, Fiz. Elem. Chastits At. Yadra **7**, 1038 (1976) [Sov. J. Part. Nucl. **7**, 415 (1976)].
[42] F. M. Bernthal and J. O. Rasmussen, Nucl. Phys. **101**, 513 (1976).
[43] I. Hamamoto, J. Holler, and X. Z. Zhang, Phys. Lett. B **226**, 17 (1989).
[44] M. K. Balodis *et al.*, Izv. Akad. Nauk SSSR, Ser. Fiz. **52**, 2117 (1988).

This article was published in English in the original Russian journal. It is reproduced here with the stylistic changes by the Translation Editor.